Clay Minerals, (2015) **50**, 497–523

Chlorite and chloritization processes through mixed-layer mineral series in low-temperature geological systems – a review

D. BEAUFORT[1,*], C. RIGAULT[1], S. BILLON[1], V. BILLAULT[1], A. INOUE[2], S. INOUE[3] AND P. PATRIER[1]

[1] *IC2MP, CNRS-UMR 7285, Hydrasa, University of Poitiers, Bâtiment B35, 6 Rue Michel Brunet, TSA 51106, 86073 Poitiers Cedex 9, France*
[2] *Department of Earth Sciences, Chiba University, 263-8522 Chiba, Japan*
[3] *Department of Earth and Planetary Science, Graduate School of Science, The University of Tokyo, 7-3-1 Hongo, Bunkyo-ku, Tokyo, 113-0033, Japan*

(*Received 20 February 2015; revised 17 August 2015; Associate Editor: Eric Ferrage*)

ABSTRACT: This present study provides an overview of the clay-mineral reactions involved in the chloritization process in a mixed-layer mineral series, and focuses on the properties of the resulting low-temperature chlorites (formed at <220°C) in diagenetic and hydrothermal systems. According to the literature, most chlorite species occurring in low-temperature geological systems are derived from specific clay precursors except for direct precipitates from solution in veins. In addition, three main types of clay-mineral series have been associated with these chloritization processes: saponite-to-chlorite, berthierine-to-chlorite and kaolinite-to-sudoite reactions. The conversion of saponite to chlorite results in the most common sequence of trioctahedral clay minerals related to the occurrence of Mg-Fe trioctahedral chlorite in a wide variety of hydrothermal and diagenetic to very low-grade metamorphism environments. Two models were proposed in the literature to describe the saponite-to-chlorite conversion through corrensite. The first model is a continuous transition model based on solid-state transformation (SST) mechanisms and is valid in rock-dominated systems (closed micro-systems with very low fluid-rock ratios). The second model is a stepwise transition model based on dissolution-crystallization mechanisms (DC) and is efficient in fluid-dominated systems (open systems with high fluid-rock ratio). The berthierine to Fe-chlorite transition results in a sequence of trioctahedral phases which are related to chloritization processes in iron-rich and reducing environments. This transformation is a cell-preserved phase transition dominated by a SST mechanism that operates simultaneously in different domains of the parental mineral and may be considered as a polymorphic mineral reaction. Finally, the conversion of kaolinite to sudoite (Al-Mg di-trioctahedral chlorite) has not been documented like the other two aforementioned conversion series. Despite the scarcity of detailed investigations, the conversion of kaolinite to sudoite through tosudite is considered a stepwise mineral reaction that is dominated by a DC mechanism. From a compilation of literature data, it appears that several parameters of hydrothermal and diagenetic chlorites differ, including the minimal temperature, the textural and structural characteristics and the extents of compositional fields. In hydrothermal systems, discrete chlorite occurs at a minimal temperature near 200°C, regardless of its chemical composition. In diagenetic systems, discrete chlorite occurs at minimal temperatures that vary according to its crystal chemistry (100–120°C for Mg-chlorite as opposed to 40–120°C for Fe chlorite). The strong discrepancy between the lowest temperature at which Mg- and Fe-chlorite form in buried sediments and in geothermal systems should result from drastically different heating rates, heat-flow

---

* E-mail: daniel.beaufort@univ-poitiers.fr
DOI: 10.1180/claymin.2015.050.4.06

conditions and tectonism between basins at passive margins and geothermal systems at active margins. The morphology, structure and compositional fields of the diagenetic Fe-rich chlorite may have been inherited from those of the berthierine precursor. All of the chlorite species formed through the DC mechanism have good geothermometry potential. However, the SST mechanism in which berthierine is transformed into chlorite could have unexplored consequences regarding the use of the chemistry (including stable isotope composition) of diagenetic Fe-chlorite for reconstructing the burial history of sediments. Further investigations regarding the formation mechanisms of mixed-layer minerals are required to provide us with insight to understand the chloritization process in low-temperature geological systems.

KEYWORDS: Low-temperature chlorite, chloritization process, reaction mechanism, mixed-layer mineral series, hydrothermal systems, diagenesis.

INTRODUCTION

Chlorite is unstable under the physicochemical conditions of the Earth's surface but can form over a wide range of temperatures in the subsurface of geological systems. Indeed, chloritization processes are considered effective from 40°C during sandstone diagenesis (Hillier & Velde, 1991) to 600°C in high-grade metamorphic rocks (Vidal *et al.*, 2001). Low-temperature chlorite (i.e. chlorite which forms at temperatures of <220°C) is a common mineral in rocks that have experienced hydrothermal or diagenetic processes. Within the last 30 y many contributors have attempted to use chlorite as a geothermometer to reconstruct the thermal histories of basins or fossil hydrothermal systems. Chemical geothermometers were proposed using two different simple, empirical calibrations. The first calibration was based on tetrahedral Al or the octahedral occupancy of trioctahedral chlorites as a function of the temperature measured in natural systems (Cathelineau & Nieva, 1985; Kranidiotis & MacLean, 1987; Jowett, 1991). The second calibration was based on thermodynamic calculations of equilibrium conditions for chlorites, the composition of which is expressed as the activities of the end-member components of known thermodynamics properties (Walshe, 1986; Vidal *et al.*, 2001, 2005; Inoue *et al.*, 2009; Bourdelle *et al.*, 2013). Recently, the use of chemical geothermometers has been extended to di-trioctahedral chlorite (Lanari *et al.*, 2014). Other geothermometers use the structural parameters derived from X-ray diffraction (XRD) peak profiles of chlorite, such as crystal order or polytype (Árkai, 1991; Walker, 1993; Merriman & Peacor, 1999; Merriman, 2005; and references therein). However, despite numerous contributions on the topic, the reliability of the chlorite geothermometers remains in question when applied to low-temperature geological environments (De Caritat *et al.*, 1993; Jiang *et al.*, 1994; Essene & Peacor 1995). None of the existing geothermometers can provide reliable results over the entire range of thermal conditions at which chlorite occurs in natural systems (De Caritat *et al.*, 1993; Vidal *et al.*, 2001; Inoue *et al.*, 2009). Many contributors have addressed the difficulty of obtaining accurate clay mineral thermometers in low-temperature geological environments. These difficulties generally include: (1) difficulties in obtaining experimental measurements of the thermodynamic properties of the clay minerals at low temperatures; and (2) the fact that clay minerals may be metastable in natural low-temperature systems. In such low-temperature systems, clay minerals do indeed react in response to kinetic factors, such as time, the fluid/rock ratio, the nature of the starting material and the transformation mechanisms (Essene & Peacor, 1995). Morse & Casey (1988) argued that a basic reason for the occurrence of metastable phyllosilicates is the existence of a continuous series of intermediate chemical/structural states between the clay minerals that are metastable at the lowest temperatures and those that form under stable equilibrium conditions at high temperatures according to the principle of the Ostwald Step Rule.

Even if chlorite is the end member of the transformations of Al-bearing trioctahedral clays with increasing temperature, it should be made clear that chloritization (i.e. the formation of discrete chlorite) does not consist of the transformation of only one mineral precursor (i.e. trioctahedral smectite) based on a unique reaction mechanism (Worden & Morad, 2003). Several precursors and several reaction schemes can form chlorite. Some problems still persist in the determination of the crystallization process of low-temperature chlorites (Inoue *et al.*, 2009). Thus, it is necessary to improve our knowledge regarding the influence of reaction mechanisms on crystal structure and chemistry, which are currently used as palaeotemperature markers in low-temperature chlorites.

The present study provides an overview of the clay-mineral reactions involved in chloritization processes through different mixed-layer mineral series, and focuses on the properties of the resulting chlorites. In addition, the relationships between chemistry and existing structural models are compared, and attempts are made to identify the mechanism that best describes the chloritization processes in diagenetic and hydrothermal systems. Finally, potential limitations of using chlorite as a palaeo-condition marker in low-temperature geological environments are discussed.

CLAY-MINERAL SERIES RELATED TO CHLORITIZATION PROCESSES AND REACTION MECHANISMS

Three main clay-mineral series are associated with the chloritization processes in low-temperature environments: (1) saponite-to-chlorite; (2) berthierine-to-chlorite; and (3) kaolinite-to-sudoite.

The conversion of saponite to chlorite

This transformation results in the most common sequence of trioctahedral clay minerals related to chloritization in a wide variety of environments, including (1) hydrothermal alterations in continental and marine environments (Inoue *et al.*, 1984; Bettison & Schiffman, 1988; Inoue & Utada, 1991; Beaufort & Meunier 1994; Buatier *et al.*, 1995; Schmidt & Robinson, 1997; Alt, 1999; among many others), and (2) diagenesis and very low-grade metamorphism (Hillier, 1993; Jiang & Peacor, 1994; Dalla Torre *et al.*, 1996; Schmidt & Livi, 1999).

Saponite is by far the most common variety of trioctahedral smectite and crystallizes at the lowest temperatures in andesitic to basaltic rocks. However, a sequence exists between low-charge saponite and high-charge vermiculite (Schiffman & Staudigel, 1995; Merriman & Peacor, 1999). As the temperature increases (or the burial depth increases during diagenesis), saponite is replaced by corrensite, which is replaced by Mg-Fe chlorite with increasing grade. Corrensite can be described as a 1:1 regular interstratification (R1) of 15 Å trioctahedral smectite (saponite) or vermiculite layers with 14 Å trioctahedral chlorite. However, several authors have suggested that corrensite which is unique in structure and composition, may be interstratified with chlorite (Beaufort *et al.*, 1997; Roberson *et al.*, 1999; Drits *et al.*, 2011; Kogure *et al.*, 2013). Thus, corrensite should be considered a single phase with a specific aggregate morphology, crystal-structure, chemical composition and discrete stability field (Shau & Peacor, 1992; Beaufort & Meunier, 1994; Beaufort *et al.*, 1997; Murakami *et al.*, 1999; Vidal *et al.*, 2012). Using XRD, high-resolution transmission electron microscopy (HRTEM) and analytical electron microscopy (AEM) analyses, Beaufort *et al.* (1997) investigated the phase relationships between corrensite, saponite and Mg-chlorite and demonstrated that the corrensite-to-chlorite reaction proceeds through mixed-layers of chlorite-corrensite, which can be distinguished from chlorite-smectite mixed-layers based on their XRD patterns (Fig. 1).

Two models have been proposed to describe the conversion of saponite to chlorite through corrensite. The first model (Chang *et al.*, 1986; Bettison & Shiffman, 1988; Bettison-Varga *et al.*, 1991; Bevins *et al.*, 1991) suggests a continuous increase in the percentage of chlorite layers within the parental smectite material as the burial depth or temperature increases. Thus, the mineral reaction proceeds gradually through a continuous series of mixed-layer chlorite-smectites in which the specific structure (i.e. the stacking sequence of both smectite and chlorite along the *c** axis) can be explained in terms of the layer stacking probability. In such a model, corrensite is a particular type of mixed-layer chlorite-smectite (i.e. regularly ordered interstratification 1:1 of trioctahedral smectite with trioctahedral chlorite). In the second model, the saponite-to-chlorite conversion progresses stepwise from saponite to corrensite and from corrensite to chlorite in the absence of randomly interstratified chlorite-smectite (C-S) (Inoue *et al.*, 1984; Inoue & Utada, 1991; Shau & Peacor, 1992; Beaufort *et al.*, 1997; Schmidt & Robinson, 1997; Murakami *et al.*, 1999). In such a conversion series, the phase relationships between the three discrete Mg-rich phyllosilicates and mixed-layer phases are viewed as mixed layers of smectite-corrensite or corrensite-chlorite (Schiffman & Staudigel, 1995; Beaufort *et al.*, 1997; Murakami *et al.*, 1999; Kogure *et al.*, 2013).

Solid-state transformation (SST) is the dominant reaction mechanism proposed in the first model for the conversion of smectite to chlorite during low-temperature diagenetic processes. Generally, SST mechanisms involve the gradual replacement of the parental mineral (saponite) with daughter mineral (Mg,Fe-chlorite) in close topotactic contact. The SST mechanism proceeds in the presence of aqueous fluids, which act as catalysts and transport media (Veblen, 1992) and influence the structure and composition of the daughter minerals (Baronnet, 1992). Phyllosilicate reactions according to the SST mechanism result in volume-conservative reactions with similar shapes and sizes of the parental

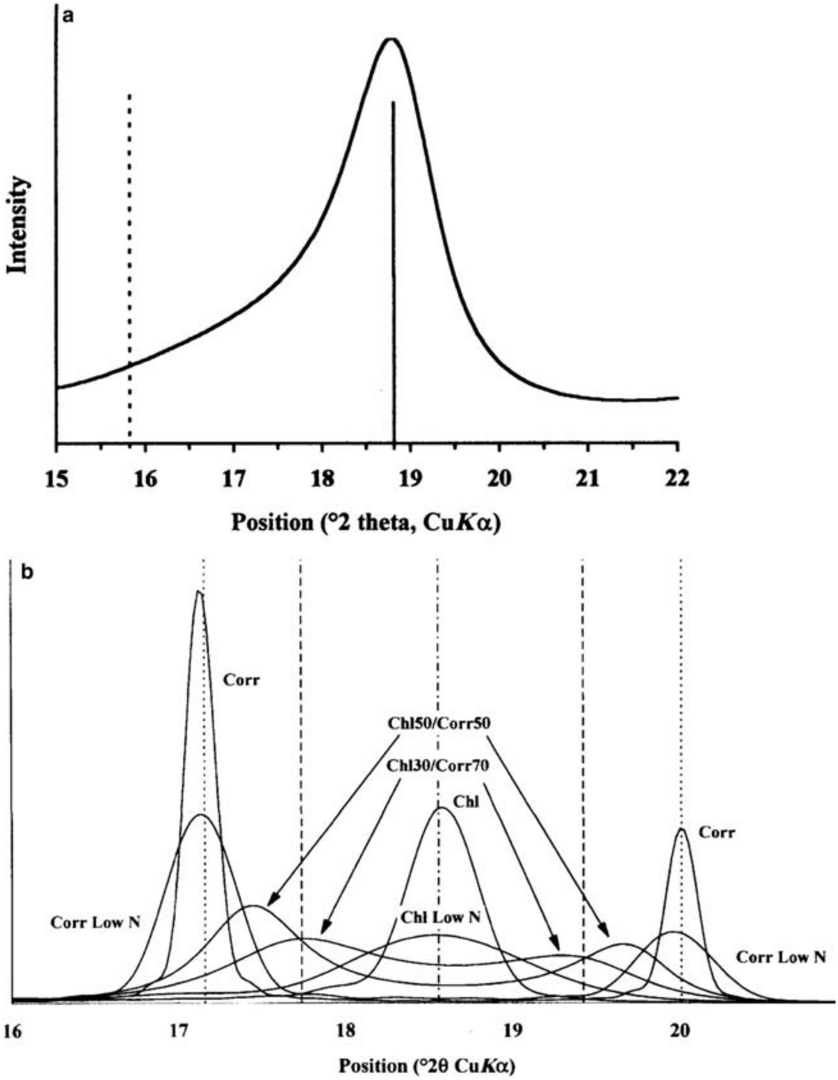

FIG. 1. Comparison between the NEWMOD simulation of the XRD patterns of the ethylene glycol-solvated chlorite-smectite and chlorite-corrensite mixed layers near the chlorite 003 reflection position. (a) Randomly oriented chlorite-smectite (75:25). The dashed line depicts the peak of the saponite 003 reflection and the solid line shows the position of the chlorite 003 reflection. (b) Chlorite, corrensite and randomly interstratified chlorite-corrensite with different proportions of each component (arrows). The parameters used for the simulations were given by Beaufort *et al.* (1997). Corr = corrensite, Chl = chlorite. Dashed lines show the positions of elementary lines associated with the corrensite (short dash), chlorite-corrensite mixed layer (long dash), and chlorite (irregular dash). Coherent scattering domain size ranges from 5 to 15 layers, except for low-N chlorite and low-N corrensite for which it ranges from 3 to 6.

and daughter plates. In addition, phyllosilicate reactions are concomitant with gradual chemical changes proportional to the extent of chloritization and with gradual structural changes (interlayer ordering and polytype). In the presence of randomly interstratified chlorite-smectite, Bettison-Varga & Mackinnon (1997) proposed that half of the 2:1 layer of saponite dissolves during the reaction while the other half is preserved.

Dissolution-crystallization (DC) is the dominant reaction mechanism proposed in the second model for smectite-to-chlorite conversion. In the extreme case of the process, this mechanism involves complete dissolution of saponite, followed by nucleation and growth of the daughter minerals as separate or epitaxial grains. In this DC mechanism, the structural memory of the saponite is lost, and the progress of the reaction may be marked by abrupt changes in chemical and structural properties, and by major changes in crystal texture (Table 1). In addition, Ostwald ripening (OR) which can be considered a particular type of DC mechanism that follows the initial nucleation stage of clay crystals has been proposed as a mechanism for chloritization processes (Jahren, 1991; Grigsby, 2001). During OR the smallest crystals dissolve and nucleate on larger preexisting crystals and at the end of the process, large crystals produced by OR are found in the authigenic core of a grain surrounded by progressively younger epitaxial overgrowths (Baronnet, 1982).

Chlorite pseudomorphs of precursor minerals also proceed according to a DC reaction mechanism but result in daughter minerals in which the structural memory of the precursor is not completely lost. Indeed, according to Putnis (2002), pseudomorphism operates by epitaxial growth at the fluid–solid interface that moves into the parent crystals. The fact that dissolution and crystallization fronts remain very close throughout pseudomorphic alteration results in the retention of some structural and textural properties of the dissolved parent minerals, and the occurrence of transient porosity in the precipitated product. Shau & Peacor (1992) argued that the continuous transition model (equivalent to SST) is only valid for chloritization processes in rock-dominated systems (closed micro systems with very low fluid-rock ratios) such as shale, in which most of the chlorite may be a by-product of smectite illitization. However, the stepwise transition model (equivalent to DC) is efficient for chloritization processes that operate in fluid-dominated systems (open systems with high fluid-rock ratios). Previously, several results from nanostructural investigations of the conversion of saponite to chlorite by HRTEM have supported the model based on dissolution-crystallization (Shau & Peacor, 1992; Beaufort *et al.*, 1997; Murakami *et al.*, 1999).

The conversion of berthierine to chlorite

This reaction involves a sequence of trioctahedral phases at low temperatures in iron-rich environments. Berthierine is an Al,Fe-rich 1:1 trioctahedral layer silicate that belongs to the serpentine group. Despite differences in the arrangements of tetrahedral and octahedral sheets resulting in periodicities along the *c* axis of ~7 Å and ~14 Å, berthierine and chlorite have similar basic structures. The stoichiometry of berthierine is the same as that of chlorite and its chemical composition overlaps with that of the ferrous chlorite endmember, chamosite (Xu & Veblen, 1996). Consequently, the conversion of berthierine to chamosite may occur through a polymorphic mineral reaction. However, because of their similar crystal structure and stoichiometry, it is difficult to characterize the interstratification of chlorite and berthierine using classical XRD or chemical analyses. Theoretical XRD simulations of chlorite/berthierine mixed layers (Reynolds, 1988; Reynolds *et al.*, 1992; Moore & Reynolds, 1997) have shown that interstratification of the 7 Å and 14 Å layers results in XRD patterns in which the odd order reflections are broad and have a weak intensity relative to the even order reflections (Figure 2). Reynolds *et al.* (1992) proposed an equation for estimating the percentage of interstratified 7 Å layers that uses full width at half maximum (FWHM) of 004 and 005 reflections, and which is valid from ~1 to 20% interstratified 7 Å layers.

The mineral reactions by which 7 Å layers (serpentine or berthierine) are progressively replaced by 14 Å layers (chlorite) are dominated by a SST mechanism (Banfield & Bailey, 1996; Xu & Veblen, 1996; Ryan & Reynolds, 1997). Based on the lateral transition from 7 Å to 14 Å layers observed by HRTEM (e.g. Banfield *et al.*, 1994; Banfield & Bailey, 1996; Xu & Veblen, 1996), the transformation of serpentine or berthierine to chlorite appears to be a cell-preserving phase transition (even though fluids play an important role as catalysts for the transformation), which simultaneously operates in different domains of the parental mineral. Because the primary difference between berthierine and chlorite structures is the arrangement of their tetrahedral and octahedral sheets, the chlorite structure can be produced from berthierine by simply reversing half of the tetrahedral sheets in the berthierine structure. Such a reversal of the tetrahedral sheet can be obtained by cross shifting Si and O atoms between two adjacent berthierine layers (Fig. 3). As the temperature increases, chloritization progresses laterally and vertically in each domain and nearly all of the pairs of original layers of serpentine are transformed progressively into chlorite layers (Hillier, 1994). Banfield & Bailey (1996) and Xu & Veblen (1996) specified that the final chlorite mineral is expected to show specific microstructures such as antiphase domain structures with odd numbers of berthierine layers between the chlorite domains. Under

TABLE 1. Predicted trends in the texture, microstructure and chemistry of the resulting minerals as chloritization proceeds according to the SST and DC mechanisms (modified from Baronnet, 1992).

	Solid-state transformation (SST) mechanism	Dissolution-crystallization transformation mechanism (DC)
Crystal habit	Conserved	Lost
Inheritance of polytypes	Yes	No
Chemical/structural heterogeneity	No	Yes
Inheritance of chemistry	Yes	No
Inheritance of defects	Yes	No

such conditions, the interstratification of berthierine layers in the Fe-chlorite particles is not thermodynamically stable because they correspond to defects created by the SST transformation mechanism. A major criticism of this structural model is that it does not explain the electrostatic difference that is supposed to exist between the two octahedral sheets (i.e. the octahedral sheet of the 2:1 layer and the interlayer brucite-like octahedral sheet) of chlorite. Indeed, in the theoretical structure of the trioctahedral chlorite, the excess electric charge that compensates for the negative charge on the tetrahedral sheets is located

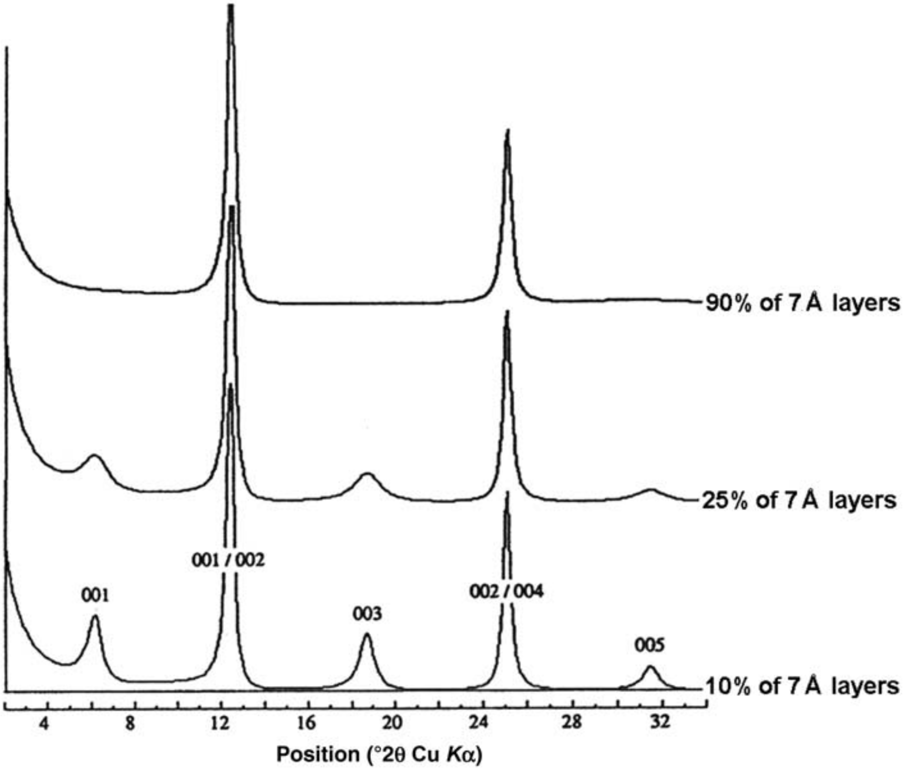

FIG. 2. Simulated XRD patterns of berthierine-chlorite mixed layers with different percentages of 7 Å layers (from Moore & Reynolds, 1997). 001/002 and 002/004 correspond to peaks resulting from the d_{001} contribution of berthierine and d_{004} of chlorite, respectively.

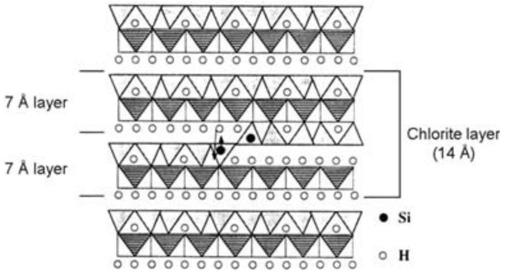

FIG. 3. Structural model of transformation from the serpentine structure to the chlorite structure. The inversion of the orientation of a tetrahedral sheet from a 1:1 layer to the previous structure is obtained by shifting the Si and H atoms (reproduced, with the permission of Springer, from Xu & Veblen, 1996).

preferentially in the brucite-like interlayer sheet (Bailey, 1988a). Further studies of the distribution of cations in the octahedral sheets of iron-rich chlorite are necessary to verify this transformation.

The conversion of kaolinite to sudoite

This last transformation is much less documented in diagenesis than the two previous conversion series. Sudoite, ideally $(Mg_2Al_3)[AlSi_3O_{10}]$ $(OH)_8$, is a di-trioctahedral chlorite with a dioctahedral sheet in the 2:1 layer and a trioctahedral interlayer sheet (Bailey, 1980). Except for examples of Palaeoproterozoic unconformity-related uranium deposits in which the precipitation of massive sudoite has been reported (Percival & Kodama, 1989; Beaufort *et al.*, 2005), these types of di-trioctahedral chlorite are seldom formed below 250°C and are limited to Al-rich geological systems in which sudoite is associated with tosudite and kaolinite.

According to the Association Internationale Pour l'Etude des Argiles (AIPEA), tosudite is defined as a 1:1 regularly interstratified chlorite-smectite that differs from corrensite because it is dioctahedral (Bailey, 1982). The dioctahedral nature is suggested by a total octahedral occupation of between 6 and 7 (based on $O_{20}(OH)_{10}$) and by d_{060} values of between 1.490 and 1.506 Å. This dioctahedral nature results in the combination of di-dioctahedral chlorite (donbassite) with either dioctahedral or trioctahedral smectite, and in combinations of dioctahedral smectite with di-trioctahedral chlorite (sudoite). Consequently, the tosudite denomination includes the clay minerals previously defined as dioctahedral corrensite (Morrisson & Parry, 1986). Several occurrences of tosudite have been reported in sedimentary (Wilson, 1971; Morrisson & Parry, 1986; Garvie, 1992; Hillier *et al.*, 2006, Billon, 2014) and hydrothermal systems (Creach *et al.*, 1986; Merceron *et al.*, 1988; Daniels and Altaner, 1990; Inoue, 1995; Bartier *et al.*, 2008; among others). The association of tosudite with dioctahedral or di-trioctahedral chlorite was mentioned in most of the aforementioned studies.

Although Hillier *et al.* (2006) interpreted kaolinite, tosudite and sudoite from the Devonian Old Red Sandstones as parts of a conversion series, no studies of possible mechanisms of the transition of kaolinite to sudoite under diagenetic conditions were reported. Recent studies have proposed beidellite as an alternative precursor to sudoite in Rotliegend sandstones from the eastern region of the southern Permian Basin (Biernacka, 2014). The absence of any documented occurrences of dioctahedral random mixed-layered chlorite-smectite in association with tosudite, and the presence of mixed chlorite-tosudite mixed layers (Fig. 4) in association with tosudite in sandstones from the Tim Mersoi basin in Niger (Billon, 2014) suggest the occurrence of stepwise mineral reactions dominated by a DC mechanism, similar to that discussed previously for the conversion of saponite to chlorite.

OCCURRENCES OF LOW-TEMPERATURE CHLORITES IN GEOTHERMAL SYSTEMS

Chlorite is a common mineral product of hydrothermal alteration of igneous rocks, volcanics and volcanogenic sediments. In addition, chlorite is considered to be an index mineral in several alteration facies in porphyry copper and geothermal systems (Lowell & Guilbert, 1970; Henley & Ellis, 1983; Pirajno, 1992). Propylitic alterations are symptomatic of thermally controlled processes that are driven by heat transfer to the rocks surrounding igneous intrusions during their cooling history (Lowell & Guilbert, 1970; Berger & Velde, 1992; Inoue, 1995). Propylitic alteration is pervasively distributed in large rock volumes without long-distance transport of cations released from the dissolution sites. According to the rock chemistry, hydrothermal paragenesis consists of trioctahedral chlorite (±corrensite) associated with variable amounts of epidote, quartz, alkali feldspars or illite (± mixed-layer illite-smectite) and/or various types of carbonates according to the bulk-rock chemistry of the protolith (Beaufort *et al.*, 1990; Berger & Velde, 1992; Mas *et al.*, 2006). Phyllic alterations (or sericitic

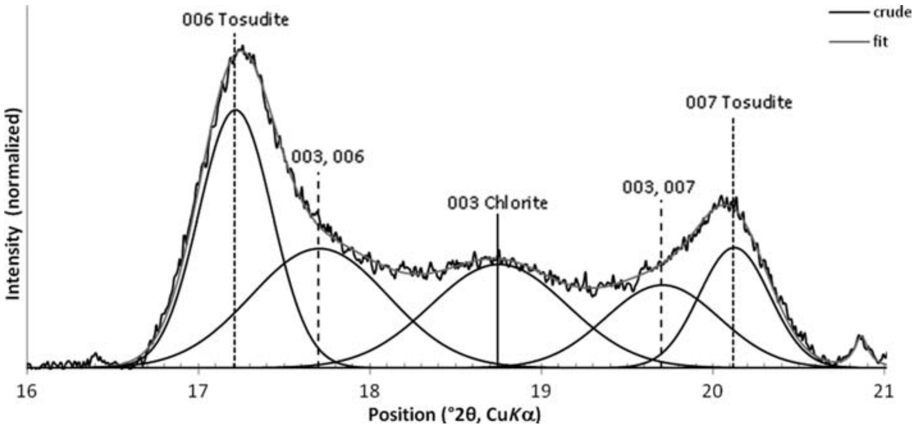

FIG. 4. Decomposition of the peak near the chlorite 003 position of an ethylene glycol-solvated sample of sandstone from the Tim Mersoi basin. The solid line depicts the position of the chlorite 003 reflection, the short dashed lines depict the 006 and 007 reflections of tosudite, and the long dashed lines depict the positions of the chlorite-tosudite mixed layer (Billon, unpublished data). 003,006 and 003,007 correspond to peaks resulting from the interference between the d_{003} reflection of chlorite and d_{006} of tosudite, and between d_{003} of chlorite and d_{007} of tosudite, respectively.

alteration) are symptomatic of open systems with mass and heat transfers through a fracture-controlled permeable network. Phyllic alteration results from the infiltration of low-pH hydrothermal fluids, which provides the H^+ ions necessary for phyllosilicate crystallization (Hemley & Jones, 1964). Even when aluminous dioctahedral phyllosilicates (phengite, illite ± mixed-layer illite-smectite minerals) are dominant in the phyllic facies, chlorite (± corrensite) occurs as veins or veinlet-filling products (Beaufort & Meunier, 1983; Beaufort *et al.*, 1990). Most low-temperature hydrothermal chlorites consist of Mg-Fe trioctahedral species, which are frequently associated with corrensite and chlorite-smectite or corrensite-smectite mixed layers (Inoue *et al.*, 1984; Inoue & Utada, 1991; Meunier *et al.*, 1991; Beaufort & Meunier, 1994; Alt, 1999). Sudoite is a common di-trioctahedral chlorite species in hydrothermal systems (Hayashi & Oinuma, 1964; Sudo & Sato, 1966; Percival & Kodama, 1989) although it is generally present in small amounts. The only type of hydrothermal system in which sudoite has been reported in large amounts and in large volumes of

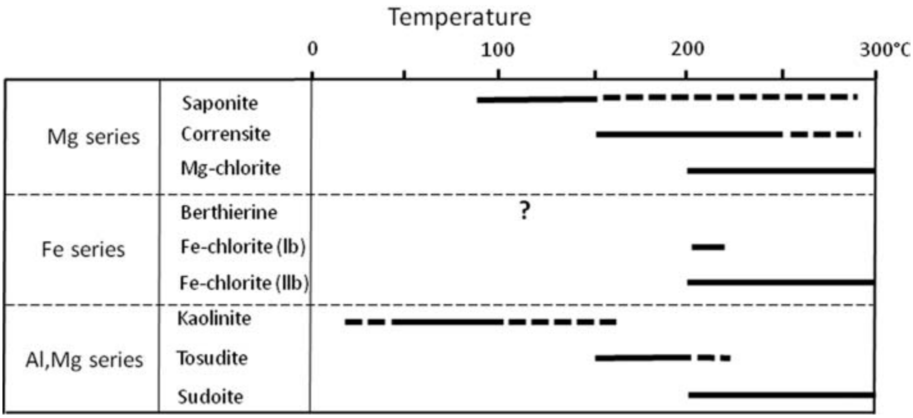

FIG. 5. Thermal ranges of the occurrence of clay minerals involved in the hydrothermal chloritization process (estimated from literature data).

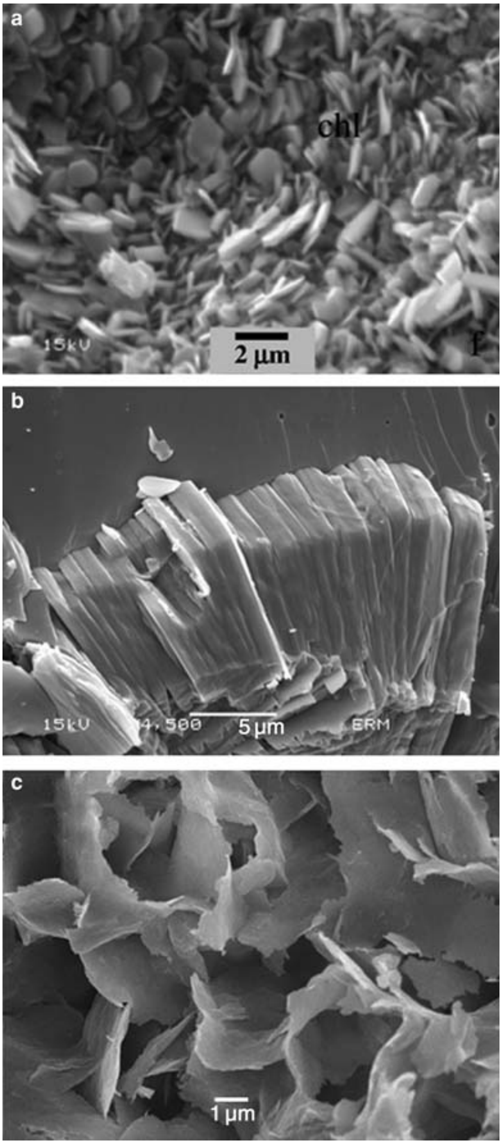

FIG. 6. Specific morphological aspects of chlorites from hydrothermal systems as a function of their crystal-chemical properties: (a) Mg-Fe rich chlorite from the geothermal field of Bouillante (reproduced, with the permission of Elsevier, from Mas *et al.*, 2006); (b) Fe-rich chlorite vermicules (chamosite) from the massive sulfide of Rouez (Rigault, unpublished data); and (c) sudoite from the Athabasca Basin, Canada (from Billault *et al.*, 2002 (figure 2a). Reproduced with the kind permission of The Clay Minerals Society, publisher of *Clays and Clay Minerals*).

altered rocks are unconformity-related uranium deposits (Percival & Kodama, 1989; Billault *et al.*, 2002; Beaufort *et al.*, 2005).

Thermal range of mineral reactions

The thermal ranges of the main clay minerals involved in the hydrothermal chloritization processes are summarized in Fig. 5. In geothermal systems, trioctahedral chlorites usually crystallize as discrete phases at temperatures >200°C (Kristmannsdottir, 1978; Henley and Ellis, 1983; Bettison & Schiffman, 1988; Beaufort *et al.*, 1992; Inoue, 1995). As previously specified, most hydrothermal chlorites in shallow geothermal systems have an Fe/(Fe + Mg) ratio (XFe) <0.5. Below 200°C, chlorite layers are interstratified with expandable trioctahedral layers (smectite, vermiculite or corrensite) to form mixed-layer minerals in which the chlorite components generally increase as the temperature increases, which agrees with thermal control of the progress of the saponite-to-chlorite transformation. Saponite and regularly ordered mixed-layer chlorite-smectite (tosudite and corrensite) occur over a wide range of thermal conditions in geothermal systems. Saponite usually occurs at low temperatures <100°C and has been observed at temperatures as high as 300°C (e.g. Schiffman & Fridleifsson, 1991; Beaufort *et al.*, 1995a,b; Patrier *et al.*, 1996; Teklemariam *et al.*, 1996; Gianelli *et al.*, 1998) particularly in deep boiling zones and in experiments with supercritical water (Vidal *et al.*, 2012). In the Nesjavellir geothermal field (Iceland), mixed-layer C-S and corrensite are the predominant layer silicates between 245 and 265°C whereas chlorite is the most abundant clay mineral with minor C-S mixed layers at higher temperatures (see Schiffman & Fridleifsson, 1991 and references therein). In active hydrothermal systems (i.e. geothermal systems), the first appearance of corrensite occurs at temperatures of between 150 and 250°C and the presence of corrensite has been noted at temperatures of up to ~300°C (Schiffman & Fridleifsson, 1991; Shau & Peacor, 1992; and references therein). Regarding the relative stability of corrensite and chlorite, Barrenechea *et al.* (2000) suggested that besides thermal control, redox conditions could significantly control the phase relationships (i.e. corrensite appears to crystallize under more oxidizing conditions than chlorite). The importance of the R^{3+} contents of corrensite and chlorite was noted by Brigatti & Poppi (1984). However, the experimental synthesis of Fe-rich corrensite under reducing conditions (Sugimori *et al.*, 2008) indicates that corrensite can form across a wide range of redox conditions. Fe-rich chlorite occurs at temperatures greater than 200°C during phyllic alteration (Beaufort *et al.*, 1992) and in epithermal polymetallic vein-type ore deposits (Shikazono & Kawahata, 1987). Berthierine appears to be restricted to sulfide-bearing veins, submarine massive sulfide deposits and hydrothermally altered shales (Smith & Hardy, 1981; Yau *et al.*, 1988, Walker & Thompson, 1990; Slack *et al.*, 1992). In addition, the occurrence of interstratified minerals that include Fe-rich chlorite layers has not been documented in detail in hydrothermal systems. Hydrothermal tosudite has been reported to form at temperatures up to 200°C (Daniels & Altaner, 1990; Bartier *et al.*, 2008). Sudoite replaced tosudite at estimated temperature of >200°C in several hydrothermal environments (Hayashi & Oinuma, 1964; Percival & Kodama, 1989; Daniels & Altaner, 1990). The polytype of the hydrothermal chlorites is probably the IIb ($\beta = 97°$)-type, which is the most abundant polytype for natural chlorites. The same polytypic stacking sequence has been identified in the chlorite-like layers of corrensite units from mixed-layer corrensite-chlorite (Kogure *et al.*, 2013). However, Fe-rich chlorite with the Ib ($\beta = 90°$) polytype has been identified in the ore-mineralized zone of the Toyoha geothermal system (Japan). The formation temperature was estimated to be 220°C according to chlorite geothermometry (Inoue *et al.*, 2010).

Textural characteristics

In geothermal systems, the size and morphology of the clay minerals involved in saponite-to-chlorite transitions were altered significantly as the chloritization process progressed. Highly folded thin films of saponite present honeycomb arrangements, flakes of corrensite show a boxwork pattern oriented perpendicular to the substratum surface, and chlorite shows packets of individual crystals with basal faces that typically present subhedral morphologies (Beaufort *et al.*, 1997). At higher temperatures (near 250°C), the chlorite crystals show a sub-hexagonal morphology (Fig. 6a), and Fe-rich chlorite crystals become coarser by thickening along the *c** axis, resulting in blockier and more rigid hexagonal plates that are often arranged in vermicular aggregates (Fig. 6b). Hydrothermal sudoite is fine grained with corn-flake morphology and is arranged in boxwork patterns oriented perpendicular to the wall-rock surface or flakes parallel to the wall-rock surface (Fig. 6c).

Crystal chemistry of hydrothermal chlorites

When plotted in an ^{VI}Al-Fe-(Mg + Mn) graph (Fig. 7a) the chemical composition of hydrothermal trioctahedral chlorites cited from the literature forms a continuous compositional field that spreads from Fe- to Mg- end-members of chlorite. In addition, a compositional gap exists between the trioctahedral and di-trioctahedral chlorites. At the local scale, the chemical composition of the trioctahedral chlorites is controlled to a significant extent by bulk-rock chemistry and phase relationships with coexisting minerals. Trioctahedral chlorite presents a low XFe when it is associated with iron oxides or sulfides (Beaufort & Meunier, 1983; Beaufort *et al.*, 1992; Milu *et al.*, 2004; Hezarkhani, 2006), an intermediate XFe when associated with epidotes (Beaufort *et al.*, 1992; Teklemariam *et al.*, 1996; Gianelli *et al.*, 1998) and a high XFe when crystallized in Fe-rich reducing rocks without sulfides (López-Munguira *et al.*, 2002). In oxidizing environments, Mg-rich chlorite (clinochlore) prevails (Beaufort *et al.*, 1992).

When plotted in the Si^{4+} *vs*. R^{2+} graph (Fig. 7b), which was proposed by Wiewióra and Weiss (1990), the structural formulae of the chlorites were similar to the theoretical trioctahedral end-member. The octahedral occupancies varied between 5.75 and 6.00 atoms per half unit cell (aphuc). The elongated extension of the compositional field of trioctahedral chlorites tends towards a theoretical end-member, which is comparable to amesite $(Mg_2Al)[AlSiO_5](OH)_4$, and resulted from the substitution of Al^{3+} for Si^{4+} in the tetrahedral sites of the Fe-rich chlorites. Several authors have indicated that increasing ^{IV}Al is correlated with an increase in ^{VI}Fe in chlorite from low-grade metamorphic rocks (Shirozu, 1978; Kranidiotis & MacLean, 1987; Bailey, 1988a; Nutt, 1989). Shau & Peacor (1992) explained these trends as a crystal-chemical response to the distortion of the chlorite lattice due to increasing amounts of Fe^{2+} in the octahedral sheets. Because the substitution of larger Fe^{2+} ions for smaller Mg^{2+} in the octahedral sheets results in dilation of the octahedral sheets, the substitution of larger ^{IV}Al for smaller Si increases the size of the tetrahedral sheets, compensating for the misfit between the octahedral and tetrahedral sheets of Fe-rich chlorites. From the ^{VI}Al-Fe-(Mg + Mn)

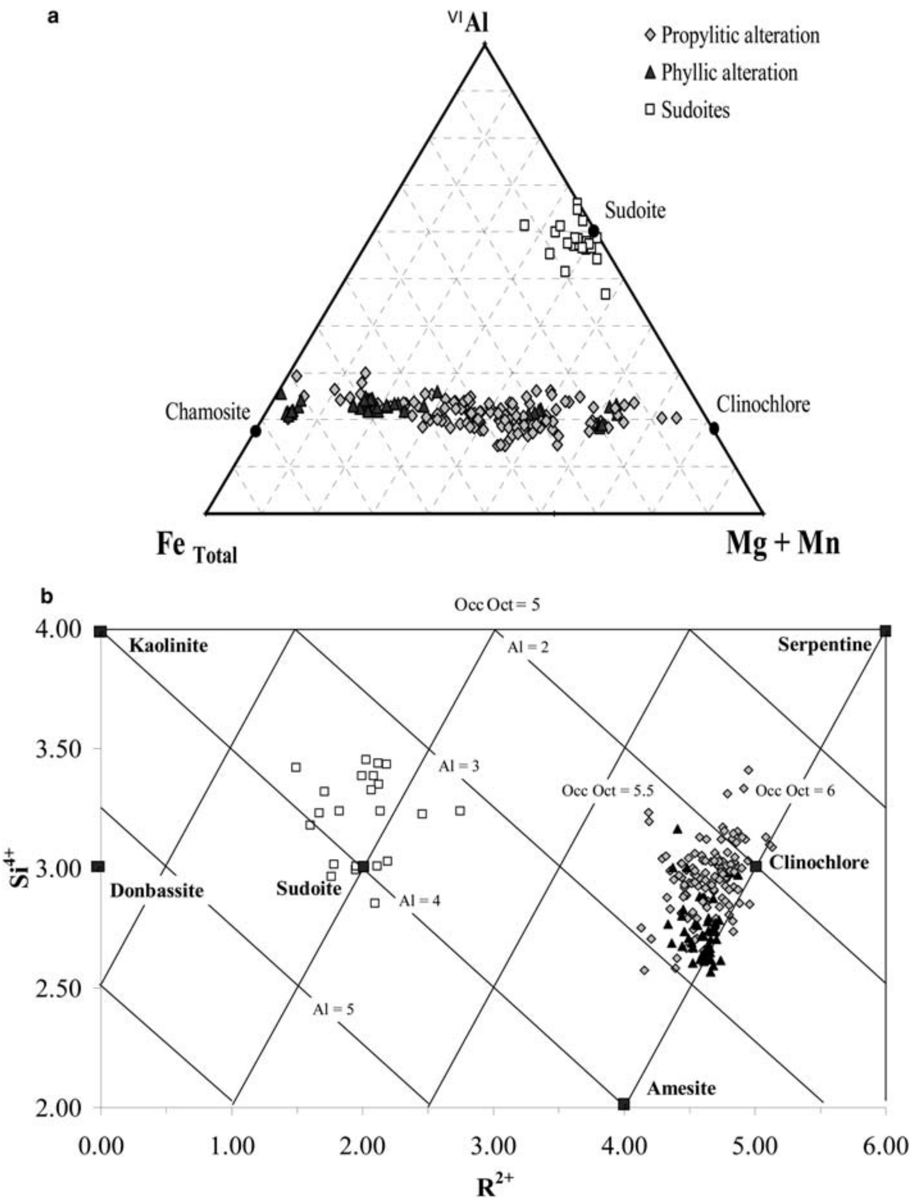

FIG. 7. Projection of the structural formulae of chlorites from hydrothermal systems in a ^{VI}Al-Fe$_{total}$-(Mg + Mn) triangular diagram (a) and Si^{4+} *vs.* R^{2+} (b) as used by Wiewióra & Weiss (1990). Data are expressed in atoms per half unit cell. Occ Oct = octahedral occupancy. Al = total number of Al atoms per half unit cell. Grey circles: trioctahedral chlorites from propylitic alteration, black triangles: trioctahedral chlorites from phyllic alteration and white squares: sudoite from various hydrothermal systems. Analyses of the trioctahedral chlorites crystallized during propylitic alterations were obtained from Bettison & Schiffman (1988), Keith & Bargar (1988), Marignac (1988), Shau *et al.* (1990), Norman *et al.* (1991), Beaufort *et al.* (1992), Teklemariam *et al.* (1996), Bettison-Varga & Mackinnon (1997), Gianelli *et al.* (1998), López-Munguira *et al.* (2002), Martínez-Serrano (2002), Hezarkhani (2006) and Mas *et al.* (2006). Analyses of the trioctahedral chlorites crystallized during phyllic alteration were obtained from Beaufort & Meunier (1983), Marignac (1988), Milu *et al.* (2004) and Hezarkhani (2006). Analyses of sudoites are from Drits & Lazarenko (1967), Kimbara & Nagata (1974), Alysheva *et al.* (1977), Fransolet & Bourguignon (1978), Sudo & Shimoda (1978), Kramm (1980), Lin & Bailey (1985), Percival & Kodama (1989), Anceau (1992) and Billault *et al.* (2002).

triangle (Fig. 7a), increasing substitution of Fe for Mg is also correlated with small increases in ^{VI}Al indicating that increasing XFe in chlorite is correlated with increasing amounts of Al in both tetrahedral and octahedral sites. The interpretation of these crystal chemical trends in trioctahedral chlorite is limited by a lack of data regarding the number of Fe^{3+} ions in the chlorite structure. Indeed, another explanation could be that ^{IV}Al is correlated with Fe^{3+} through a Tschermak-type substitution: $^{VI}Al\ Fe^{3+} = Si\ (Mg, Fe^{2+})$.

From the chemical compositions collected in the literature, hydrothermal sudoite does not significantly deviate from its ideal composition (Fig. 7b). Instead, these sudoites are characterized by greater Si content than trioctahedral chlorite (between 3.00 and 3.45 aphuc) and an octahedral occupancy that is near the ideal value of di-trioctahedral chlorite (i.e. 5.00 aphuc). In the absence of intimate mixing with dioctahedral phyllosilicates, the small compositional deviations of natural sudoite from ideal endmembers result from Tschermak substitution and iron substitution at the two different octahedral sites (Fe^{3+} for Al, Fe^{2+} for Mg and $2Fe^{3+}$ for 3Mg). Because use of Mössbauer spectroscopy indicated that the iron involved in these substitutions is predominantly ferric, increasing the amount of iron in sudoite generally shifts its compositional field towards the dioctahedral endmember (Billault *et al.*, 2002).

OCCURRENCES OF LOW-TEMPERATURE CHLORITES IN DIAGENETIC SYSTEMS

Although chlorite results from the burial diagenetic transformation of precursor minerals (Worden & Morad, 2003; and reference therein), its occurrence requires sedimentary pre-requisite material essential for forming chlorite precursor clay phases such as saponite, glauconite, berthierine and odinite. Most Fe-rich chlorites occur in coastal environments while Mg-rich chlorites occur in marine and terrestrial sandstones (Dowey *et al.*, 2012 and references therein). Thus, two distinctive clay-mineral series have been related to the occurrence of trioctahedral chlorites under diagenetic conditions (Hillier, 1994; Worden & Morad, 2003), the magnesian series, which results in trioctahedral chlorite with Fe/(Fe + Mg) (XFe) < 0.5 (referred to hereafter as Mg-rich chlorite), and the ferroan series, which results in trioctahedral chlorite with XFe > 0.5 (referred to hereafter as Fe-rich chlorite).

The magnesian series involves the depth-dependent conversion of saponite to Mg-rich chlorite. This mineral transition proceeds *via* corrensite with mixed-layer minerals in combination with layer arrangements of the aforementioned clay minerals. The conversion of saponite to chlorite has been described in the burial diagenesis of lacustrine mudrocks or limestones (Hillier, 1993; Barrenechea *et al.*, 2000), shales (Chang *et al.*, 1986) or sandstones (Tompkins, 1981; Hillier, 1994; Humphreys *et al.*, 1994), and is effective in very low-grade metamorphism of pelitic rocks (Merriman & Peacor, 1999 and reference therein). The ferroan series involves the depth-dependent replacement of Al and Fe-rich serpentine-like minerals (7 Å layers) by Fe-rich chlorite (14 Å layers) through mixed-layer serpentine-like-chlorite intermediates. Grain-coating and pore-lining Fe-rich diagenetic chlorite frequently occurs in sandstones deposited at the transition between marine and fluvio-deltaic environments (verdine facies environment). Odinite and berthierine are both considered the most likely mineral precursors for the formation of Fe-rich chlorite (chamosite), and chloritization proceeds through a series of mixed-layer chlorite-berthierine minerals with increasing burial depth (Kisch, 1983; Ahn & Peacor, 1985; Bailey, 1988b; Odin, 1988, 1990; Ehrenberg, 1990, 1993; Walker & Thompson, 1990; Hillier, 1994; Hornibrook & Longstaffe, 1996; Ryan & Reynolds, 1996; Aagaard *et al.*, 2000; Ryan & Hillier, 2002).

Berthierine is a very common clay mineral that is present in modern sediments and Fe-rich sedimentary rocks (Rohrlich *et al.*, 1969; French, 1973; Bhattacharyya, 1983; Van Houten & Purucker, 1984; Maynard, 1986; Hornibrook & Longstaffe, 1996). Berthierine generally occurs as pore-linings, pore-fillings, peloids, and detrital mineral-replacement features (Ryan & Reynolds, 1996). It is an Fe-rich phyllosilicate that is formed from the interactions of the most reactive detrital Al-Fe minerals with sedimentary solutions under reducing conditions (Velde, 1985) and/or affects the ingestion of sediments by macro-organisms (Peyraud & Worden., 2007) before the earliest stage of burial diagenesis. In shallow-marine environments in tropical regions at temperatures as low as 25°C, the occurrence of berthierine can be preceded by odinite (Porrenga, 1967), which is a poorly crystallized di-trioctahedral Fe^{3+}-rich phyllosilicate with a serpentine-like structure (Bailey, 1988b; Odin, 1988). Several studies have documented the occurrence of sudoite in burial diagenesis (Schultz, 1963; Anceau, 1992; Hillier, *et al.*, 2006; Biernacka, 2014); however, the reaction pathway by which sudoite forms in basins remains unknown. Otherwise, simulations of the XRD profiles indicate that sudoite layers are also formed in the reacting mixed-layer illite-smectite, resulting in three-component mixed-layer illite-smectite-sudoite within the shales of the Texas Gulf Coast (Lanson *et al.*, 2009).

Thermal range of mineral reactions

The thermal ranges of the main clay minerals involved in the diagenetic chloritization processes are summarized in Fig. 8. Diagenetic chlorites are formed at much lower temperatures than in hydrothermal systems. Mg-rich chlorite (clinochlore) replaces corrensite at temperatures above 100–120°C (Worden & Morad, 2003; and references therein), and tosudite and corrensite are formed at temperatures of <100°C which is before the formation of chlorite (Morrison & Parry, 1986; Hillier, 1993; Worden & Morad, 2003; Hillier *et al.*, 2006). Based on the vitrinite reflectance data, Chang *et al.* (1986) estimated that corrensite can occur at temperatures as low as 60°C in sandstones and as low as 70°C in shales. Ryan & Hillier (2002) and Worden & Morad (2003) indicated that corrensite is also stable at higher temperatures (90–120°C in sandstones). Even when chlorites are interstratified with smectites, referred to as "swelling chlorites" (Curtis *et al.*, 1985), no specific variations of the crystal structure occur between the diagenetic and the hydrothermal chlorites that result from the saponite-to-chlorite transformation process. Despite a much lower crystallization temperature, the diagenetic Mg-rich chlorites have the IIb ($\beta = 97°$) polytype.

The temperature at which Fe-rich chlorite replaces berthierine is still debated, but several studies have indicated that the conversion of berthierine to Fe-rich chlorite can be achieved at much lower temperatures than the conversion of saponite to Mg-chlorite under diagenetic conditions. According to several authors, Fe-rich chlorite occurs near the transition between eogenesis and mesogenesis at temperatures ranging from 40 to 120°C (Ehrenberg, 1990; Aagaard *et al.*, 2000; Worden & Morad, 2003, and references therein). The XRD patterns of the Fe-rich diagenetic chlorites are characterized by mixed-layered chlorite-berthierine containing a small number of berthierine layers (Billault, 2002; Ryan & Hillier, 2002). High-resolution transmission electron microscopy fringe images confirm the presence of 7 Å layers interlayered with 14 Å layers in the chlorite domains, and give microstructural evidence of the lateral conversion of 7 Å layers to 14 Å chlorite layers (Fig. 9). The Fe-rich chlorite that results from the diagenetic transformation of berthierine is the Ib ($\beta = 90°$) polytype (Hillier, 1994; Billault, 2002; Ryan & Hillier, 2002). The low-temperature limit at which sudoite replaces tosudite in diagenetic systems has not been documented. The crystallization of sudoite in low-grade aluminous metapelites is restricted to temperatures of >200°C (Fransolet & Schreyer, 1984; Franceschelli *et al.*, 1989; Theye *et al.*, 1992; Vidal *et al.*, 1992).

Textural characteristics

Mg-rich and Fe-rich diagenetic chlorites can be distinguished based on their textural characters (Hillier, 1994). Mg-rich chlorite frequently occurs as pore linings and grain coatings of detrital quartz. Chlorite coatings consist of platelets with cornflake-like morphology that are arranged in a boxwork texture that could be inherited from the textural properties of parental corrensite (Fig. 10a,b). Fe-rich diagenetic chlorites occur as euhedral platy crystals with pseudo-hexagonal habits. These chlorites can be arranged as individual plates or rosettes (Fig. 10c,d) and constitute quartz-grain coatings that protect the pore space of sandstones from quartz cementation (Hillier, 1994; Ryan & Hillier, 2002; Billault *et al.*, 2003). Only a few descriptions of tosudite and sudoite have been reported for sandstone reservoirs (Garvie, 1992; Biernacka, 2014; Billon, 2014). The most frequent modes of occurrence of tosudite and sudoite appear to be as grain coatings and pore linings that form typical honeycomb textures (Fig. 10e,f).

Crystal chemistry of diagenetic chlorites

When plotted in two graphs of ^{VI}Al-Fe-(Mg + Mn) and Si^{4+}-R^{2+}, the compositional field of the diagenetic chlorites is widespread compared with that for hydrothermal chlorites (Fig. 11a,b). The compositional field of the diagenetic chlorites deviates from that of theoretical trioctahedral chlorite (i.e. from full occupation of the octahedral sites) by a significant increase in the number of octahedral vacancies, indicating a trend towards the di-trioctahedral end-member. However, two distinctive chlorite populations can be distinguished.

The chemical compositions of diagenetic Mg-rich chlorites (IIb polytype) that originate from the saponite-to-chlorite transformation do not differ significantly from the hydrothermal chlorites formed by that transformation. Their compositional field is near the theoretical trioctahedral end-member (mean octahedral

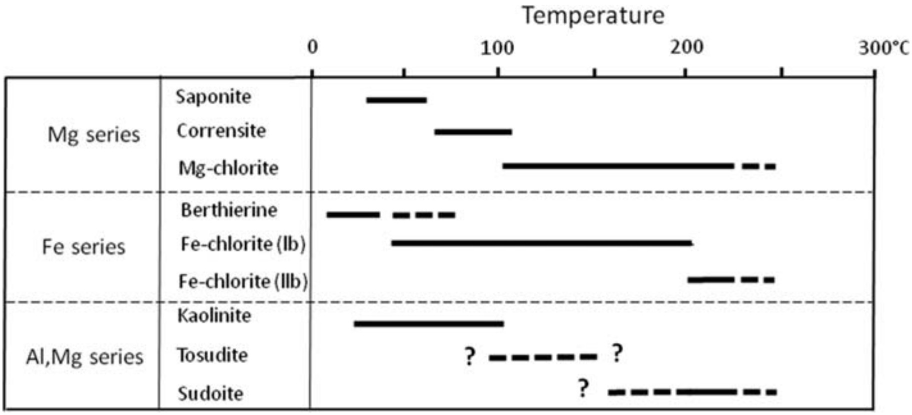

FIG. 8. Thermal ranges of the occurrence of clay minerals involved in diagenetic chloritization processes (estimated from literature data).

occupancy near 5.80 aphuc) and they have a relatively wide range of Al-for-Si substitutions in tetrahedral sheets (Si content varying from 2.57 to 3.26 aphuc). Diagenetic Fe-rich chlorites that crystallize from berthierine precursors are chemically different from hydrothermal Fe-rich chlorites. These chlorites are much more heterogeneous in composition and can be differentiated by greater Al contents and greater numbers of octahedral vacancies. The Al^{VI} content varies from 0.98 to 2.01 aphuc, with a mean value of 1.55. In addition, the Al^{IV} content varies from 0.88 to 1.43 aphuc, with a mean value of 1.14. Their octahedral occupancy varies from 5.25 to 6.00 aphuc, with a mean value of ~5.60 atoms. Ryan & Hillier (2002) noted a positive correlation between the percentage of berthierine layers and the Fe/(Fe + Mg) ratio that was measured in the diagenetic Fe-rich chlorites. It is unclear, however, whether the causes of these variations are related to the temperature of the chloritization reaction or chemical heterogeneity of

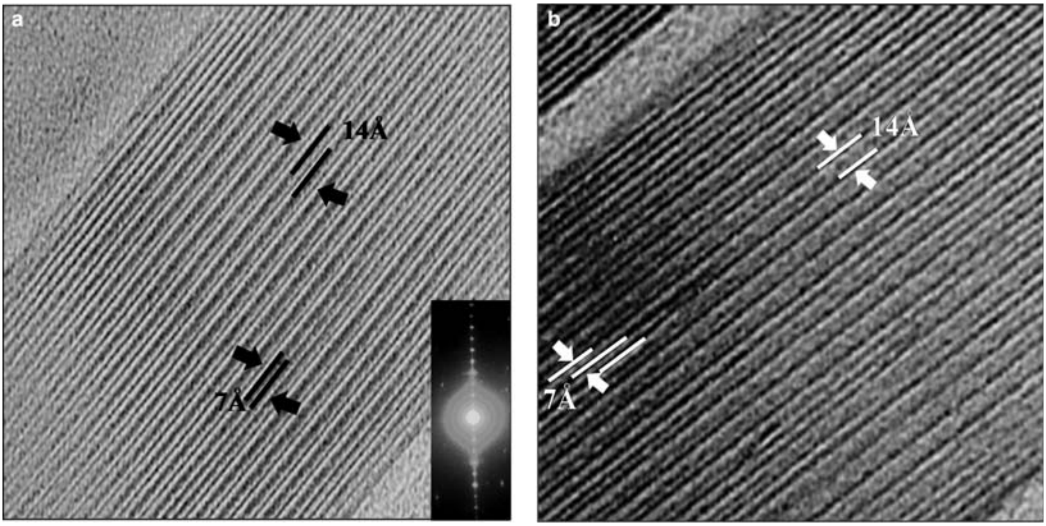

FIG. 9. HRTEM lattice imaging of a Fe-rich diagenetic chlorite: (a) the presence of residual 7 Å layers as defects in the final chlorite structure; and (b) the lateral transition from two 7 Å layers to one 14 Å chlorite layer in a berthierine-chlorite mixed-layer mineral. These microstructures are relevant to the transformation of berthierine to chlorite through a solid-state mechanism (Billault, 2002, reproduced with the author's permission, from his PhD thesis).

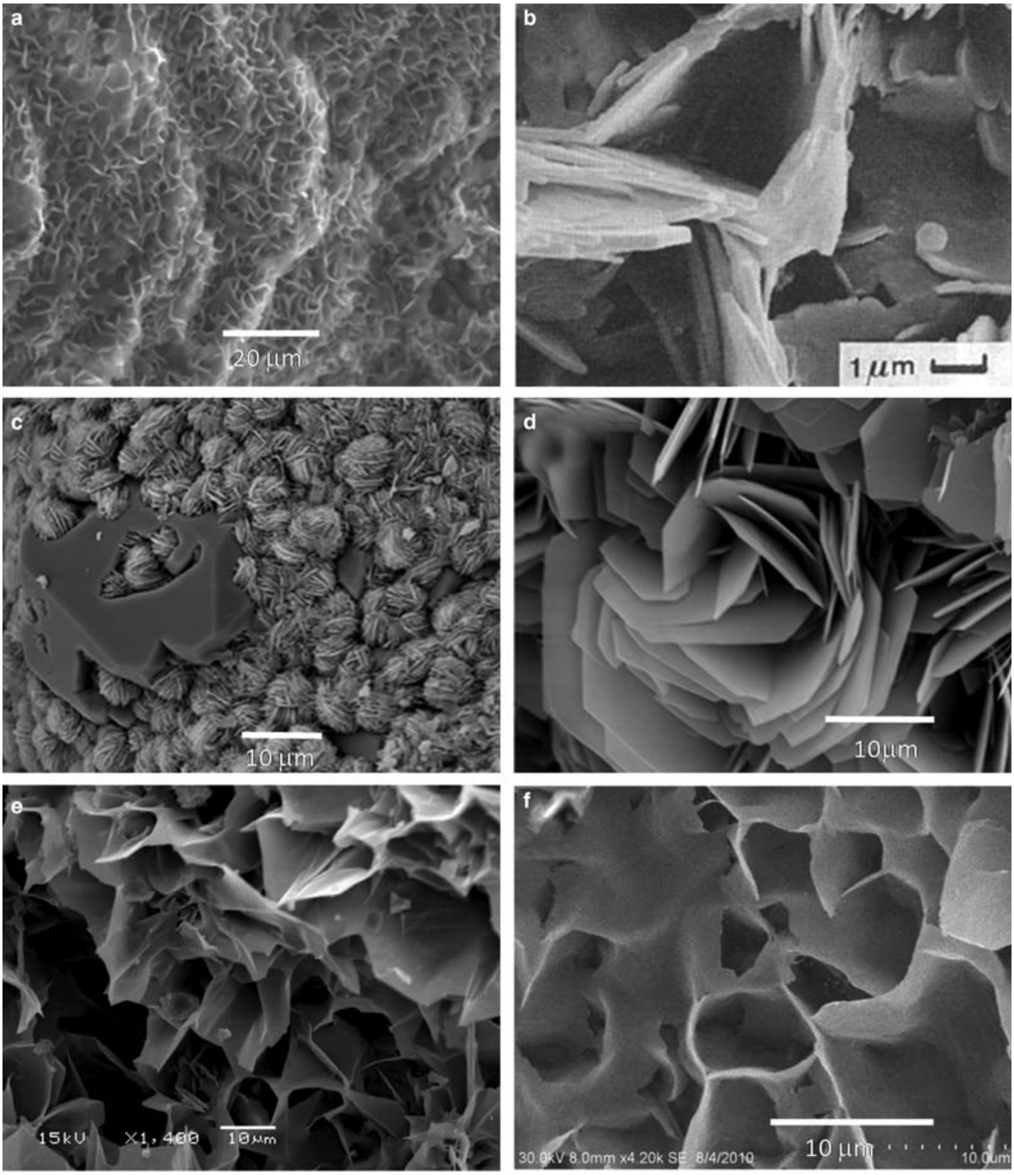

FIG. 10. Morphological aspects of diagenetic corrensite, chlorites and tosudite formed in sandstone reservoirs. (a) Corrensite grain coating with a typical honeycomb arrangement of flakes (Rainoldi, unpublished data); (b) Mg-Fe rich chlorite with cornflake-like morphology (Hillier, 1994); (c) Fe-rich chlorite resulting from the transformation of berthierine into chlorite arranged in rosettes (Rigault, unpublished data); (d) Fe-rich chlorite resulting from the transformation of berthierine into chlorite arranged in euhedral platy crystals with pseudo-hexagonal habits (Beaufort, unpublished data); (e) grain-coating tosudite with a honeycomb flake arrangement (Billon, unpublished data); and (f) pore-lining sudoite (reproduced from Biernacka, 2014).

the precursor material. Despite the heterogeneity, the chemistry of diagenetic chlorites shows a positive correlation between increasing substitution of Fe-for-Mg and increasing amounts of Al in tetrahedral and octahedral sheets, suggesting a deviation toward a di-trioctahedral compositional pole. The compositional

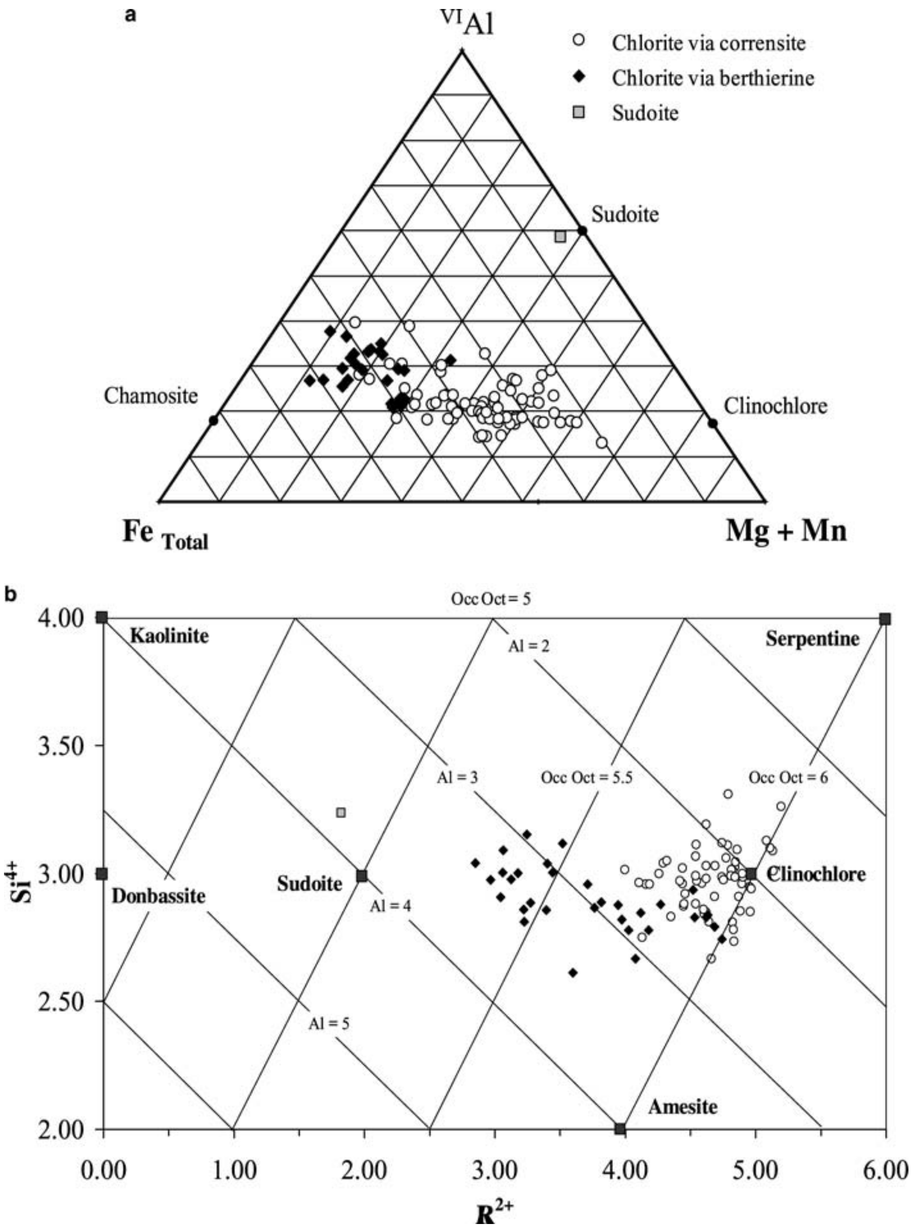

FIG. 11. Projection of the structural formulae of chlorites from diagenetic systems in (a): ^{VI}Al-Fe$_{total}$-(Mg + Mn) triangular diagram, and (b) Si^{4+} *vs.* R^{2+} as used by Wiewióra & Weiss (1990). Data are expressed in atoms per half unit cell. Black diamonds: trioctahedral Fe-rich chlorites resulting from berthierine-to-chlorite transformation; white circles: trioctahedral Mg-rich chlorites resulting from saponite-to-chlorite transformation; grey square: sudoite from bentonite. Data from the Mg-rich chlorites from Humphreys *et al.* (1989), Hillier & Velde (1991), Hillier (1993, 1994), and Barrenechea *et al.* (2000). Data from the Fe-rich chlorites are from Curtis *et al.* (1985), Whittle (1986), Hillier (1994), Xu &Veblen (1996), Billault (2002) and Ryan & Hillier (2002), and the datum from sudoite is from Anceau (1992). Other labels units are as in Fig. 7.

variations of diagenetic sudoite have not been documented in the literature.

DISCUSSION

In the debate on the validity of proposed chlorite geothermometers, it has been suggested that difficulties calibrating such geothermometers for chlorites formed in diagenetic or low-temperature geothermal systems (Hayes, 1970; Walshe, 1986; Vidal *et al.*, 2001) result from their compositional (Curtis *et al.*, 1985; Hillier & Velde, 1991) and structural variations (Hayes, 1970; Walker, 1993), issues that do not affect geothermometers calibrated for higher-grade metamorphic chlorites. Instead of addressing the respective deficiencies of the different chlorite geothermometers in low-temperature geological environments, the goal of the present study was to better identify the causes of the wide range of compositional and structural variations exhibited by chlorites formed at low temperature, and to improve our understanding of the relationship between these variations using the transformation mechanisms that best describe chloritization in such environments.

The summary presented here suggests that many of the specific crystallochemical properties of natural chlorites formed at low temperatures are influenced by factors other than the temperatures at which the chloritization reactions proceed. The major characteristics of the chlorites studied in hydrothermal and diagenetic environments are summarized in Table 2 as functions of different parameters, such as the nature of the mineral precursor, the type of the conversion series, the lowest temperature of occurrence of discrete chlorite, the nature of the predominant mechanism of chloritization, and the inferred consequences of these properties for the potential use of the chemical and structural properties of these chlorites as indicators of the thermal history of low-temperature geological systems.

On the thermodynamic status of the clay minerals involved in the chloritization processes

From a compilation of data in the literature, it appears that most chlorite species that occur in low-temperature geological systems are derived from specific clay precursors. The formation of chlorite from the transformation of a clay-mineral precursor through a series of intermediate products is likely because it requires low activation energy and is kinetically more likely (Putnis, 1992; Merriman, 2005). Thus, the transformation series, and the kinetically controlled formation of intermediate products following the Ostwald Step Rule (Fig. 12), could explain the chemical heterogeneity of low-temperature chlorite particles which result in mixtures of chlorite and intermediate mixed-layer phases (corrensite, mixed-layer chlorite-corrensite, mixed-layer chlorite-berthierine …) which may persist because of an incomplete transformation process.

The thermodynamic status of these intermediate mixed-layer phases has given rise to much debate and is a source of some controversy in relation to thermodynamic stability or metastability in both diagenetic and hydrothermal environments. There is indeed a vast literature which argues that the mixed-layer minerals involved in the clay series which follow the qualitative Ostwald step rule are metastable and that their reactions at low temperature are controlled by kinetics. In this model, which was detailed by Morse & Casey (1988), the crystallization of metastable phases is controlled by nucleation and the observed paragenetic pathways involve thermodynamically unfavoured phases which cannot be predicted from thermodynamics. According to these authors, the persistence of relatively unstable minerals can be understood in terms of standard kinetic theory, where the most rapid of a given sequence of parallel reactions controls the overall rate. Usually the quickest rate proceeds *via* metastable intermediate minerals which convert at slow rates to the thermodynamically favoured phase. An eventual metastability of the mixed-layer minerals would invalidate their use in low-temperature thermometry. On the basis on several experimental works, Vidal *et al.* (2012) suggested that the succession of different types of mixed-layer phases with changing proportions is not necessarily indicative of metastability. In such an alternative model each kind of transient phase can be understood using the concept of local equilibrium. In that case, each type of chlorite-bearing mixed-layer mineral would have precipitated only in local areas where a fluid-solid equilibrium had been reached. Chlorite might be the ultimate and stable clay mineral at the very end of the process, but not the most stable phase at any intermediate conditions of the geothermal or diagenetic history. Finally, the observed multistep reaction would not mean that the intermediate mixed-layer minerals are less stable than the chlorite end product because the local bulk composition changed with time and hence all these minerals could have potential for use in thermodynamic geothermometry. Thus far, chlorite geothermometry has never been performed on chlorite-bearing mixed-layer minerals

Table 2. Comparison between the characteristics of the hydrothermal and diagenetic chlorite in terms of the nature of their mineral precursor, the type of conversion series, the minimal temperature of occurrence and the predominant mechanism of chloritization.

Geological systems	Crystal chemistry	Conversion series	Transformation mechanism	Dominant polytype	Textural change	Minimal temp.	Chemical heterogeneity
Hydrothermal systems	Trioctahedral XFe <0.5	Saponite to chlorite *via* corrensite	DC in fluid-dominated systems SST in rock-dominated systems	IIb	Temperature-related change in size and shape	200°C	Weak
	Trioctahedral XFe >0.5	nd	DC	IIb	Temperature-related change in size and shape	200°C	Weak
	Di-trioctahedral (Al-Mg)	Kaolinite to sudoite *via* tosudite	DC	IIb	Temperature-related change in size and shape	200°C	Weak
Burial diagenesis	Trioctahedral XFe <0.5	Saponite to chlorite *via* corrensite	DC	IIb	Temperature-related change in size and shape	100°C	Moderate
	Trioctahedral XFe >0.5	Berthierine to chlorite Ib to IIb Fe-chlorite	SST DC?	Ib IIb	No textural change? Temperature-related change in size and shape	40–60°C 200°C	Strong Moderate to weak
	Di-trioctahedral (Al-Mg)	Kaolinite to sudoite *via* tosudite	DC	IIb	nd	<200°C	nd

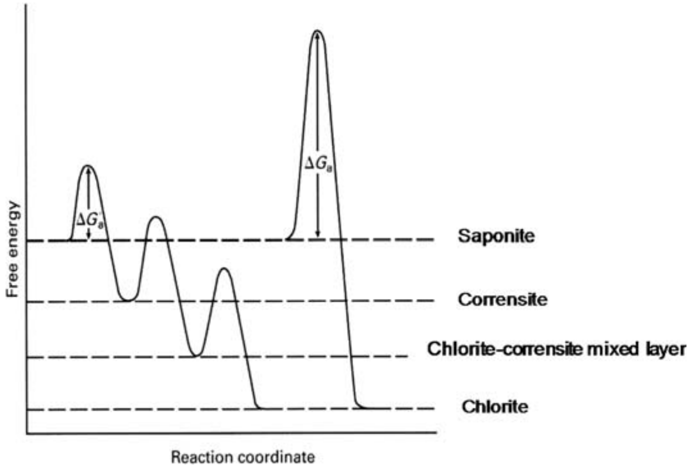

FIG. 12. Schematic diagram illustrating the Ostwald Step Rule when applied to reactants and products in the saponite-to-chlorite reaction series. Direct transformation from saponite to chlorite requires a large activation energy, ΔG_a, and is unlikely in a normal sedimentary basin setting. Transformation *via* a series of intermediate products requires smaller activation energies and is kinetically more likely in sedimentary basins (modified from Merriman, 2005).

because it requires the analysis of individual chlorite layers and the determination of the thermodynamic properties of mixed layers is not a simple problem to solve. There are pros and cons for both of the aforementioned models. Given the complexity of the tectono-thermo-hydrochemical history of hydrothermal and diagenetic systems, both models may well be valid in different parts of each of the systems. The first one seems more appropriate for interpreting the chloritization process in porous and permeable rocks which constitute the fluid reservoirs whereas the second is expected in fluid-poor environments in which the fluid composition can be changed locally during the reaction, and be heterogeneous at the microscale.

An alternative method for forming chlorite in natural systems is direct precipitation from supersaturated solutions, a process that requires high activation energy. Direct precipitation of chlorite or illite has frequently been mentioned in hydrothermal systems in which infiltrating aqueous fluids achieve greater degrees of supersaturation in terms of clay minerals at temperatures >200°C (Simmons & Browne, 2000; and references therein). In hydrothermal systems, it seems likely that clay minerals can precipitate at lower temperatures from supersaturated fluids because the large activation energies can be attained by rapid cooling of upwelling high-temperature geothermal solutions and by fracture-controlled mixing of hydrothermal fluids with different compositions and/or temperatures (Reeder, 1985). Because direct precipitation can also explain the discontinuous transformation of saponite to corrensite and corrensite to chlorite, additional investigations are necessary for providing insight regarding the formation mechanisms of chlorite and its mixed-layer relatives in low-temperature hydrothermal systems. Thus, further investigations by HRTEM will be required to identify the stacking structure and characterize the respective component layers of the interstratification from chemical and structural viewpoints. The conditions required for the direct precipitation of chlorite appear to be more difficult to reach in burial-diagenesis environments which are generally characterized by very slow heating rates.

On the chemical control of the clay precursors

The specific nature of clay precursors and clay-mineral series involved in chloritization processes at low temperatures depends on the chemical conditions of the upper portions of the Earth's crust which are summarized below. The conversion of saponite to Mg-rich chlorite occurs under oxidizing and near-neutral pH conditions such as clay diagenesis in arid environments or shallow hydrothermal systems dominated by the infiltration of sea water or meteoric fluids. In these environments, Fe precipitates mostly as ferric iron oxides or oxyhydroxides. The conversion of trioctahedral smectite to chlorite through corrensite is the prevailing 'magnesian way' of chloritization in low-temperature environments when the oxidizing conditions in the upper part of the crust are depleted in organic reducing agents, which strongly limit the availability of ferrous iron in the solutions. Ferrous trioctahedral smectite is scarce (Kohyama *et al.*, 1973) because these minerals are highly unstable at near-surface conditions (Badaut *et al.*, 1985; Parthasarathy *et al.*, 2003). Consequently, crystallization of ferroan smectite and its thermally controlled conversion to ferroan chlorite are unlikely under such conditions. Fe-rich corrensite (with XFe up to 0.94) was synthesized by Sugimori *et al.* (2008) during the experimental alteration of Fe-rich chlorite and biotite under very low f_{O_2} conditions. However, Fe-rich corrensite is not known to occur in natural systems. The conversion of berthierine to Fe-rich chlorite through a chlorite–berthierine series is the predominant method for ferroan chloritization in sandstones during the burial of fluvial and deltaic sediments (Dowey *et al.*, 2012). In such processes, authigenic berthierine is thought to have formed near the surface under rather anoxic conditions, potentially by replacing pre-existing odinite. No equivalent magnesian conversion series (e.g. amesite to clinochlore) is known to occur in diagenetic settings. Indeed, amesite is a relatively rare mineral that crystallizes at temperature and/or pressure conditions corresponding to low-grade and contact metamorphic environments (Hall and Bailey, 1976; Aagard & Jahren, 1992), and chloritization of serpentine through interstratified chlorite-serpentine minerals has been reported only in high-temperature metamorphic or hydrothermal systems (Banfield *et al.*, 1994; Banfield & Bailey, 1996). The conversion of kaolin minerals to sudoite appears to be restricted to geological environments that are influenced by the interaction of Mg-rich fluids with Al-rich sedimentary or volcanogenic rocks under relatively acidic and oxidizing conditions (Kister *et al.*, 2005). Beside the massive crystallization of sudoite observed in Proterozoic intracratonic basins, several occurrences of sudoite formed directly from kaolinite or dickite at the transition between deep diagenesis and very low-grade metamorphism have been reported (Daniels & Altaner, 1990; Ruiz Cruz & Sanz de Galdeano, 2005).

Discrepancy of the thermal range between hydrothermal and diagenetic chloritization processes

A significant discrepancy exists between the lowest temperature at which Mg- and Fe-chlorites form in buried sediments and in low-temperature hydrothermal systems. For example, the temperature at which Mg-rich chlorite forms from saponite is approximately two times greater in hydrothermal systems than in sedimentary rocks (Fig. 5, 8). This finding may be because of the different thermal histories of these two types of geological environments. Drastic differences in the heating rate, heat-flow conditions and tectonism between passive margin basins and geothermal systems at active margins largely explain the aforementioned thermal discrepancy between diagenetic and hydrothermal chlorites. As discussed by Merriman (2005), the time taken to achieve a mineral reaction (such as illitization or chloritization) in sedimentary basins ranges from 1×10^4 y in the very high heat flow geothermal system of the Salton Sea in the USA (Yau *et al.*, 1988; Velde & Lanson, 1993) to $>2 \times 10^9$ y in the Palaeoproterozoic basin of McArthur in Australia (Patrier *et al.*, 2003). Reducing the activity of water may be an important parameter which contributes to reduction of the thermal stability of expandable clay minerals in sedimentary basins (Vidal & Dubacq, 2009; Vidal *et al.*, 2012). A reduced activity of water in sedimentary fluids is expected in particular in deeply buried sedimentary rocks in which the diagenetic solutions are highly saline (brines). Moreover, at such burial depths, a further reduction in $a\text{H}_2\text{O}$ can be due to the mixing of water with other fluids or gas. However, the role of water activity in the thermal stability of the mixed-layer minerals which predated chlorite is difficult to ascertain in burial diagenesis because most of the chloritization processes occur at shallow to moderate burial depths at which we can assume that $a\text{H}_2\text{O}$ is nearly 1.

Potential role of the transformation mechanism

The literature concerning the formation of low-temperature chlorites emphasizes the importance of the transformation mechanisms in controlling the properties of diagenetic chlorites. Even if the magnesian or ferroan characteristics of diagenetic chlorite are inherited from the depositional sediment environment, the main differences between the resulting chlorites are in terms of the chemical heterogeneity, texture and crystal structure which result from the transformation mechanism. Fe-rich chlorite, which forms by a polymorphic reaction from berthierine by SST mechanism, is characterized by the Ib ($\beta = 90°$) polytype, chemical heterogeneity, structural defects, and the absence of morphological changes in the crystals with increasing temperature. (Mg,Fe)-chlorite, which results from the step-by-step replacement of trioctahedral smectite through a DC mechanism (*via* corrensite), is characterized by the IIb polytype (β = 97°), homogeneous chemical composition, and increasing crystal size with increasing temperature. Although it seems reasonable that the chemical/structural properties of chlorites formed by the DC mechanisms are controlled thermally, the effects of thermal control are not as clear for Fe-rich chlorites formed by SST mechanisms. According to the structural model of chloritization through the SST transformation of two berthierine layers into one chlorite layer proposed by Banfield & Bailey (1996) and Xu & Veblen (1996), Ib (β = 90°) Fe-rich chlorites observed in sandstone diagenesis at low temperature cannot be considered thermodynamically stable. These studies suggest that as long as the DC mechanism is not effective, the chlorite resulting from SST mechanism could retain the chemical and textural states of the parental berthierine. Thus, the Ib (β = 90°) polytype of Fe-rich chlorite inherited from SST transformation of 1 T berthierine (Xu & Veblen, 1996) could persist during burial if the chlorites are not completely replaced by IIb chlorites through the DC mechanism. According to the chlorite polytype variations with sample depth and temperature in sedimentary formations, this recrystallization is achieved at temperatures near 200°C (Walker, 1993). More comparative HRTEM data regarding the microstructure of Fe-rich chlorites from diagenetic and hydrothermal environments are required to test such hypotheses.

CONCLUSIONS

A review of the clay-mineral reactions involved in chloritization processes through mixed-layer mineral series, and the properties of the resulting chlorites in low-temperature geological systems lead us to the following conclusions:

(1) In low-temperature diagenetic and hydrothermal systems, chloritization processes consist of distinctive mineralogical sequences of clay minerals. The magnesian, ferrous or aluminous nature of these clay minerals is determined by the local geochemical conditions. The conversion of saponite to Mg-chlorite predominates in natural systems in which ferrous iron is not available for silicate reactions. The conversion of berthierine to Fe-rich chlorite occurs during the diagenesis of sediments under reducing conditions. The conversion of kaolinite to sudoite is restricted to geological environments that are subject to the interactions of Mg-rich fluids with sedimentary or volcanogenic Al-rich rocks under relatively acidic and oxidizing conditions.

(2) Two different reaction mechanisms are involved in these chloritization processes: dissolution-crystallization (DC) and solid-state transformation (SST). The DC mechanism leads to the stepwise conversion of saponite to Mg-chlorite and of kaolinite to sudoite. In addition, the SST mechanism may be responsible for the replacement of berthierine by Fe-rich chlorite at temperatures as low as 40°C.

(3) Chlorites formed by DC mechanisms are useful sources of information for the physicochemical conditions of formation. Thus, the chemical composition of the chlorite has potential for geothermometry. This does not preclude any debates regarding the respective roles of thermodynamics and kinetics. The SST mechanism by which berthierine is converted to chlorite differs from the SST model proposed for the smectite-to-illite reaction because it consists of a polymorphic reaction.

(4) The Ib polytype, which is typical of most Fe-rich chlorites encountered in diagenetic systems, results directly from the conversion of berthierine to Fe-rich chlorite through the SST mechanism. The fact that this SST mechanism is volume-conservative and preserves the chemical variability and relative positions of the octahedral sheets of the parental berthierine in the resulting chlorite could have unexplored consequences in the use of Fe-chlorite chemistry (including stable isotope composition) for reconstructing the burial history of sediments.

(5) Finally, further investigations regarding the formation mechanisms of mixed-layer minerals are required to provide us with insight to understand the chloritization process in low-temperature geological systems.

ACKNOWLEDGMENTS

The authors thanks Jeffrey Walker and Olivier Vidal for their careful and constructive reviews which improved this manuscript. This paper uses data from thesis studies supported financially by the TOTAL and AREVA companies.

REFERENCES

Aagard P. & Jahren J.S. (1992) Diagenetic illite-chlorite assemblages in arenites. II. Thermodynamic relations. *Clays and Clay Minerals*, **40**, 547–554.

Aagaard P., Jahren J.S., Harstad A.O., Nilsen O. & Ramm M. (2000) Formation of grain-coating chlorite in sandstones. Laboratory synthesized *vs*. natural occurrences. *Clay Minerals*, **35**, 261–269.

Ahn J.H. & Peacor D.R. (1985).Transmission electron microscopic study of diagenetic chlorite in Gulf Coast argillaceous sediments. *Clays and Clay Minerals*, **33**, 228–236.

Alt J.C. (1999) Very low grade hydrothermal metamorphism of basic igneous rocks. Pp. 169–201 in: *Low-Grade Metamorphism* (M. Frey & D. Robinson, editors). Blackwell Science, Oxford, UK.

Alysheva E.I., Rusinova O.V. & Chekvaidze V.B. (1977) Sudoite from polymetal deposit of Rudnyy. *Academy* of Sciences, *USSR, Doklady Earth Science Section*, **236**, 167–169.

Anceau A. (1992) Sudoite in some Visean (Lower Carboniferous) K-bentonites from Belgium. *Clay Minerals*, **27**, 283–292.

Árkai P. (1991) Chlorite crystallinity: an empirical approach and correlation with illite crystallinity, coal rank and mineral facies as exemplified by Palaeozoic and Mesozoic rocks of northeast Hungary. *Journal of Metamorphic Geology*, **9**, 723–734.

Badaut N., Besson G., Decarreau A. & Rautureau M. (1985) Occurrence of a ferrous, trioctahedral smectite in recent sediments of Atlantis II Deep, Red Sea. *Clay Minerals*, **20**, 389–404.

Bailey S.W. (1980) Structures of layer silicates. Pp. 1–123 in: *Crystal Structures of Clay Minerals and their X-ray Identification* (G.W. Brindley & G. Brown, editors). Monograph **5**, Mineralogical Society, London.

Bailey S.W. (1982) Nomenclature for regular intersratifications. *American Mineralogist*, **67**, 394–398.

Bailey S.W. (1988a) Chlorites: Structures and crystal chemistry. Pp. 347–403 in: *Hydrous Phyllosilicates (Exclusive of Micas)* (S.W. Bailey, editor). Reviews in Mineralogy, **19**, Mineralogical Society of America, Washington DC.

Bailey S.W. (1988b) Odinite, a new dioctahedral-trioctahedral Fe^{3+} rich clay mineral. *Clay Minerals*, **23**, 237–247.

Banfield J.F. & Bailey S.W. (1996) Formation of regularly interstratified serpentine-chlorite minerals by tetrahedral inversion in long-period serpentine polytypes. *American Mineralogist*, **81**, 79–91.

Banfield J.F., Bailey S.W. & Barker W.W. (1994) Polysomatism, polytypism, defect microstructures, and reaction mechanisms in regularly and randomly interstratified serpentine and chlorite. *Contributions to Mineralogy and Petrology*, **117**, 137–150.

Baronnet A. (1982) Ostwald ripening in solution. The case of calcite and mica. *Estudios Geologicos*, **38**, 185–198.

Baronnet A. (1992) Polytypism and stacking disorder. Pp. 232–288 in: *Mineral Reactions at the Atomic Scale: Transmission Electron Microscopy* (P. Buseck, editor). Reviews in Mineralogy, **27**, Mineralogical Society of America, Washington DC.

Barrenechea J.F., Rodas M., Frey M., Alonso-Azcárate J. & Mas J.R. (2000) Chlorite, corrensite, and chlorite-mica in Late Jurassic fluvio-lacustrine sediments of the Cameros basin of Northeastern Spain. *Clays and Clay Minerals*, **48**, 256–265.

Bartier D., Ledesert B., Clauer N., Meunier A., Liewig N., Morvan G. & Addad A. (2008) Hydrothermal alteration of the Soultz-sous-Forets granite (hot fractured rock geothermal exchanger) into a tosudite and illite assemblage. *European Journal of Mineralogy*, **20**, 131–142.

Beaufort D. & Meunier A. (1983) A petrographic study of phyllic alteration superimposed on potassic alteration: the Sibert porphyry deposit (Rhone, France). *Economic Geology*, **78**, 1514–1527.

Beaufort D. & Meunier A. (1994) Saponite, corrensite and chlorite-saponite mixed-layers in the Sancerre-Couy deep drill-hole (France). *Clay Minerals*, **29**, 47–61.

Beaufort D., Westercamp D., Legendre O. & Meunier A. (1990) The fossil hydrothermal system of Saint Martin (Lesser Antilles): Geology and and lateral distribution of alterations. *Journal of Volcanology and Geothermal Research*, **40**, 219–243.

Beaufort D., Patrier P., Meunier A. & Ottaviani M.M. (1992) Chemical variations in assemblages including epidote and/or chlorite in the fossil hydrothermal system of Saint Martin (Lesser Antilles). *Journal of Volcanology and Geothermal Research*, **51**, 95–114.

Beaufort D., Papapanagiotou P., Patrier P. & Traineau H. (1995a) Les interstratifiés I-S et C-S dans les champs géothermiques actifs: sont-ils comparables à ceux des séries diagénétiques? *Bulletin Centres Recherches Exploration-Production, ELF Aquitaine*, **19**, 267–291.

Beaufort D., Papapanagiotou P., Fujimoto K., Patrier P. & Kasai K. (1995b) High temperature smectites in active geothermal systems. Pp. 493–496 in: Water–Rock Interaction (Y.K. Kharaka & O.V. Chudaev, editors). Balkema, Rotterdam.

Beaufort D., Baronnet A., Lanson B. & Meunier A. (1997) Corrensite: A single phase or a mixed-layer phyllosilicate in the saponite-to-chlorite conversion series? A case study of Sancerre-Couy deep drill hole (France). *American Mineralogist*, **82**, 109–124.

Beaufort D., Patrier P., Laverret E., Bruneton P. & Mondy J. (2005) Clay alteration associated with Proterozoic unconformity-type uranium deposits in the East Alligator Rivers Uranium Field, Northern Territory, Australia. *Economic Geology*, **100**, 515–536.

Berger G. & Velde B. (1992) Chemical parameters controlling the propylitic and argillic alteration process. *European Journal of Mineralogy*, **4**, 1439–1455.

Bettison L.A. & Schiffman P. (1988) Compositional and structural variations of phyllosilicates from the Point Sal ophiolite, California. *American Mineralogist*, **73**, 62–76.

Bettison-Varga L. & Mackinnon I.D.R. (1997) The role of randomly mixed-layered chlorite/smectite in the transformation of smectite to chlorite. *Clays and Clay Minerals*, **45**, 506–516.

Bettison-Varga L., Mackinnon I.D.R. & Schiffman P. (1991) Integrated TEM, XRD and electron microprobe investigation of mixed-layer chlorite-smectite from the Point Sal ophiolite, California. *Journal of Metamorphic Geology*, **9**, 697–710.

Bevins R.E., Robinson D. & Rowbotham G. (1991) Compositional variations in mafic phyllosilicates from regional low-grade metabasites and application to the chlorite geothermometer. *Journal of Metamorphic Geology*, **9**, 711–721.

Bhattacharyya D.P. (1983) Origin of berthierine in ironstones. *Clays and Clay Minerals*, **31**, 173–182.

Biernacka J. (2014) Pore lining sudoite in Rotliegend sandstones from the eastern part of the southern Permian Basin. *Clay Minerals*, **49**, 635–655.

Billault V. (2002) *Texture, structure et propriétés cristallochimiques des chlorites ferreuses dans les réservoirs gréseux*. Thesis, University of Poitiers, France 193 pp.

Billault V., Beaufort D., Patrier P. & Petit S. (2002) Crystal chemistry of Fe-sudoites from uranium deposits in the Athabasca basin (Saskatchewan, Canada). *Clays and Clay Minerals*, **50**, 70–81.

Billault V., Beaufort D., Baronnet A. & Lacharpagne J.C. (2003) A nanopetrographic and textural study of grain-coating chlorites in sandstone reservoirs. *Clay Minerals*, **38**, 315–328.

Billon S. (2014) *Minéraux argileux dans le gisement d'Imouraren (Bassin de Tim Mersoï, Niger): implications sur la genèse du gisement et sur l'optimisation des procédés de traitement*. Thesis, University of Poitiers, France 340 pp.

Bourdelle F., Parra T., Chopin C. & Beyssac O. (2013) A new chlorite geothermometer for diagenetic to low-grade metamorphic conditions. *Contributions to Mineralogy and Petrology*, **165**, 723–735.

Brigatti M.F. & Poppi L. (1984) Crystal chemistry of corrensite: a review. *Clays and Clay Minerals*, **32**, 391–399.

Buatier M.D., Fruhgreen G.L. & Karpoff A.M. (1995) Mechanisms of Mg-phyllosilicate formation in a hydrothermal system at a sedimented ridge (Middle Valley, Juan de Fuca). *Contributions to Mineralogy and Petrology*, **122**, 134–151.

Cathelineau M. & Nieva D. (1985) A chlorite solid-solution geothermometer the Los Azufres (Mexico) geothermal system. *Contributions to Mineralogy and Petrology*, **91**, 235–244.

Chang H.K., Mackenzie F.T. & Schoonmaker J. (1986) Comparisons between the diagenesis of dioctahedral and trioctahedral smectite, Brazilian offshore basins. *Clays and Clay Minerals*, **34**, 407–423.

Creach M., Meunier A. & Beaufort D. (1986) Tosudite crystallization in the kaolinized granitic cupola of Montebras, Creuse, France. *Clay Minerals*, **21**, 225–230.

Curtis C.D., Hughes C.R., Whiteman J.A. & Whittle C.K. (1985) Compositional variation within some sedimentary chlorites and some comments on their origin. *Mineralogical Magazine*, **49**, 375–386.

Dalla Torre M., Livi K.J.T. & Frey M. (1996) Chlorite textures and compositions from high-pressure/low-temperature metashales and metagreywackes, Franciscan Complex Diablo Range, California, USA. *European Journal of Mineralogy*, **8**, 825–846.

Daniels E.J. & Altaner S.P. (1990) Clay mineral authigenesis in coal and shale from the Anthracite region, Pennsylvania. *American Mineralogist*, **75**, 825–839.

De Caritat P., Hutcheon I. & Walshe J.L. (1993) Chlorite geothermometry: a review. *Clays and Clay Minerals*, **41**, 219–239.

Dowey P.J., Hodgson D.M. & Worden R.H. (2012) Prerequisites, processes, and prediction of chlorite grain coatings in petroleum reservoirs: A review of subsurface examples. *Marine and Petroleum Geology*, **32**, 63–75.

Drits V.A. & Lazarenko E.K. (1967) Structural-mineralogical characteristics of donbassites. *Mineralog. Sbornik. L'vovsk Geol Obshchestvo*, **21**, 40–48 (in Russian).

Drits V.A., Ivanovskaya T.A., Sakharov B.A., Zviagyna B. B., Gor'kova N.V., Pokrovskaya E.V. & Savichev A.T. (2011) Mixed-layers corrensite-chlorites and their formation mechanisms in the glauconitic sandstones-clayed rocks (Riphean, Anabar uplift). *Lithology and Mineral Resources*, **46**, 566–593.

Ehrenberg S.N. (1990) Relationship between diagenesis and reservoir quality in sandstones of the Garn Formation, Haltenbanken, Mid-Norwegian Continental Shelf. *American Association of Petroleum Geologists Bulletin*, **75**, 1579–1592.

Ehrenberg S.N. (1993) Preservation of anomalously high porosity in deeply buried sandstones by grain-coating chlorite: examples from the Norwegian continental shelf. *American Association of Petroleum Geologists Bulletin*, **77**, 1260–1286.

Essene E.J. & Peacor D.R. (1995) Clay mineral thermometry – a critical perspective. *Clays and Clay Minerals*, **43**, 540–553.

Franceschelli M., Mellini M., Memmi I. & Ricci C.A. (1989) Sudoite, a rock-forming mineral in Verrucano of the northern Apennines (Italy) and the sudoite-chloritoid-pyrophyllite assemblage in prograde metamorphism. *Contributions to Mineralogy and Petrology*, **101**, 274–279.

Fransolet A.-M. & Bourguignon P. (1978) Di/trioctahedral chlorite in quartz veins from the Ardenne, Belgium. *The Canadian Mineralogist*, **16**, 365–373.

Fransolet A.M. & Schreyer W. (1984) Sudoite, di/trioctahedral chlorite – a stable low-temperature phase in the system MgO-Al_2O_3-SiO_2-H_2O. *Contributions to Mineralogy and Petrology*, **86**, 409–417.

French B.M. (1973) Mineral assemblages in diagenetic and low-grade metamorphic iron-formation. *Economic Geology*, **68**, 1063–1074.

Garvie L.A.J. (1992) Diagenetic tosudite from the lowermost St. Maughan's Group, Lydney Harbour, Forest of Dean. *Clay Minerals*, **27**, 507–513.

Gianelli G., Mekuria N., Battaglia S., Chersicla A., Garofalo P., Ruggieri G., Manganelli M. & Gebregziabher Z. (1998) Water-rock interaction and hydrothermal mineral equilibria in the Tendaho geothermal system. *Journal of Volcanology and Geothermal Research*, **86**, 253–276.

Grigsby J.D. (2001) Origin and growth mechanism of authigenic chlorite in sandstones of the lower Vicksburg Formation, South Texas. *Journal of Sedimentary Research*, **71**, 27–36.

Hall S.H. & Bailey S.W. (1976) Berthierine from Antartica. *American Mineralogist*, **61**, 497–499.

Hayashi H. & Oinuma K. (1964) Aluminian chlorite from Kamikita mine, Japan. *Clay Science*, **2**, 22–30.

Hayes J.B. (1970) Polytypism of chlorite in sedimentary rocks. *Clays and Clay Minerals*, **18**, 285–306.

Hemley J.J., & Jones W.R. (1964). Chemical aspects of hydrothermal alteration with emphasis on hydrogen metasomatism. *Economic Geology*, **59**, 538–569.

Henley R.W. & Ellis A.J. (1983) Geothermal systems ancient and modern, a geochemical review. *Earth Sciences Review*, **19**, 1–50.

Hezarkhani A. (2006) Mineralogy and fluid inclusion investigations in the Reagan Porphyry System, Iran, the path to an uneconomic porphyry copper deposit. *Journal of Asian Earth Sciences*, **27**, 598–612.

Hillier S. (1993) Origin, diagenesis, and mineralogy of chlorite minerals in Devonian lacustrine mudrocks, Orcadian Basin, Scotland. *Clays and Clay Minerals*, **41**, 240–259.

Hillier S. (1994) Pore-lining chlorites in siliciclastic reservoir sandstones: electron microprobe, SEM and XRD data, and implications for their origin. *Clay Minerals*, **29**, 665–679.

Hillier S. & Velde B. (1991) Octahedral occupancy and the chemical composition of diagenetic (low-temperature) chlorites. *Clay Minerals*, **26**, 149–168.

Hillier S., Wilson M.J. & Merriman R.J. (2006) Clay mineralogy of the Old Red Sandstone and Devonian sedimentary rocks of Wales, Scotland and England. *Clay Minerals*, **41**, 433–471.

Hornibrook E.R.C.& Longstaffe F.J. (1996) Berthierine from the lower Cretaceous Clearwater Formation, Alberta, Canada. *Clays and Clay Minerals*, **44**, 1–21.

Humphreys B., Smith S.A. & Strong G.E. (1989) Authigenic chlorite in late Triassic sandstones from the Central Graben, North Sea. *Clay Minerals*, **24**, 427–444.

Humphreys B., Kemp S.J., Lott G.K., Bermanto, Dharmayanti D.A. & Samsori I. (1994) Origin of grain-coating chlorite by smectite transformation: an example from Miocene sandstones, North Sumatra back-arc basin, Indonesia. *Clay Minerals*, **29**, 681–692.

Inoue A. (1995) Formation of clay minerals in hydrothermal environments. Pp. 268–330 in: *Origin and Mineralogy of Clays* (B. Velde, editor) Springer-Verlag, Berlin, Heidelberg.

Inoue A. & Utada M. (1989) Mineralogy and genesis of hydrothermal aluminous clays containing sudoite, tosudite, and rectorite in a drillhole near the Kamikita kuroko ore deposit, northern Honshu, Japan. *Clay Science*, **7**, 193–217.

Inoue A., Utada M., Nagata H. & Watanabe T. (1984) Conversion of trioctahedral smectite to interstratified chlorite/smectite in Pliocene acidic pyroclastic sediments of the Ohyu district, Akita Prefecture, Japan. *Clay Science*, **6**, 103–116.

Inoue A., Meunier A., Patrier-Mas P., Rigault C., Beaufort D. & Vieillard P. (2009) Application of chemical geothermometry to low-temperature trioctahedral chlorites. *Clays and Clay Minerals*, **57**, 371–382.

Inoue A., Kurokawa K. & Hatta T. (2010) Application of chlorite geothermometry to hydrothermal alteration in Toyoha Geothermal System, southwestern Hokkaido, Japan. *Resource Geology*, **60**, 52–70.

Jahren J.S. (1991). Evidence of Ostwald Ripening-related recrystallisation of diagenetic chlorites from reservoir rocks, offshore Norway. *Clay Minerals*, **26**, 169–178.

Jiang W.T., Peacor D.R. & Buseck P.R. (1994) Chlorite geothermometry: contamination and apparent octahedral vacancies. *Clays and Clay Minerals*, **42**, 593–605.

Jowett E.C. (1991) Fitting iron and magnesium into the hydrothermal chlorite geothermometer: *GAC/MAC/SEG. Joint Annual Meeting (Toronto, May 27–29, 1991), Program with Abstracts*, **16**, A62.

Keith T.E.C. & Bargar K.E. (1988) Petrology and hydrothermal mineralogy of US Geological Survey Newberry 2 drill core from Newberry Caldera, Oregon. *Journal of Geophysical Research*, **93**, 10174–10190.

Kimbara K. & Nagata H. (1974) Clay minerals in the core samples of the mineralized zone of Niida, southern part of Odate Akita Prefecture, Japan. *Japanese Association of Mineralogists, Petrologists and Economic Geologists Journal*, **69**, 239–254.

Kisch H.J. (1983) Mineralogy and petrology of burial diagenesis (burial metamorphism) and incipient metamorphism in clastic rocks. Pp. 289–493 in: *Diagenesis in Sediments and Sedimentary Rocks,* **2** (G. Larsen& G.V. Chilingar, editors). Elsevier, New York.

Kister P., Vieillard P., Cuney M., Quirt D. & Laverret E. (2005) Thermodynamic constraints on the mineralogical and fluid composition in a Proterozoic clastic sedimentary basin: the Athabasca Basin (Saskatchewan, Canada). *European Journal of Mineralogy*, **17**, 325–342.

Kogure T., Drits V.A. & Inoue S. (2013) Structure of mixed-layers corrensite-chlorite revealed by high resolution transmission elctron microscopy (HRTEM). *American Mineralogist*, **98**, 1253–1260.

Kohyama N., Shimoda S. & Sudo T. (1973) Iron-rich saponite (ferrous and ferric forms). *Clays and Clay Minerals*, **21**, 229–237.

Kramm U. (1980) Sudoite in low-grade manganese rich-assemblages. *Neues Jahrbuch fur Mineralogie Abhandlungen*, **138**, 1–13.

Kranidiotis P. & MacLean W.H. (1987) Systematics of chlorite alteration at the Phelps Dodge massive sulfide deposit, Matagami, Quebec. *Economic Geology*, **82**, 1898–1911.

Kristmannsdottir H. (1978) Alteration of basaltic rocks by hydrothermal activity at 100–300°C. Pp. 359–367 in: *Proceedings of the International Clay Conference, Oxford, 1978* (M.M. Mortland and V.C. Farmer, editors). Elsevier, Amsterdam.

Lanari P., Wagner T. & Vidal O. (2014) A thermodynamic model for di-trioctahedral chlorite from experimental and natural data in the system MgO-FeO-Al_2O_3-SiO_2-H_2O: applications to P-T sections and geothermometry. *Contributions to Mineralogy and Petrology*, **167**:968.

Lanson B., Sakharov B.A., Claret F. & Drits V.A. (2009) Diagenetic smectite-to-illite transition in clay-rich sediments: A reappraisal of X-ray diffraction results using the multi-specimen method. *American Journal of Science*, **309**, 476–516.

Lin C.Y. & Bailey S.W. (1985) Structural data for sudoite. *Clays and Clay Minerals*, **33**, 410–414.

López-Munguira A., Nieto F. & Morata D. (2002) Chlorite composition and geothermometry: A comparative HRTEM/AEM-EMPA-XRD study of Cambrian basic lavas from the Ossa Morena zone, SW Spain. *Clay Minerals*, **37**, 267–281.

Lowell, J.D. & Guilbert, J.M. (1970) Lateral and vertical alteration and mineralization zoning in porphyry ore deposits. *Economic Geology*, **65**, 373–408.

Marignac C. (1988) A case of ore deposition associated with paleogeothermal activity: The polymetallic ore veins of Aïn Barbar (NE Constantinois, Algeria). *Mineralogy and Petrology*, **39**, 107–127.

Martínez-Serrano R.G. (2002) Chemical variations in hydrothermal minerals of the Los Humeros geothermal system, Mexico. *Geothermics*, **31**, 579–612.

Mas A., Guisseau D., Patrier Mas P., Beaufort D., Genter A., Sanjuan B. & Girard J.P. (2006) Clay minerals related to the hydrothermal activity of the Bouillante geothermal field (Guadeloupe). *Journal of Volcanology and Geothermal Research*, **158**, 380–400.

Maynard J.B. (1986) Geochemistry of oolitic iron ores, an electron microprobe study. *Economic Geology*, **81**, 1473–1483.

Merceron T., Inoue A., Bouchet A. & Meunier A. (1988) Lithium-bearing donbassite and tosudite from Echassieres, Massif Central, France. *Clays and Clay Minerals*, **36**, 39–46.

Merriman R.J. (2005) Clay minerals and sedimentary basin history. *European Journal of Mineralogy*, **17**, 7–20.

Merriman R.J. & Peacor D.R. (1999) Very low-grade metapelites: mineralogy, microfabrics and measuring reaction progress. Pp. 10–60 in: *Low-Grade Metamorphism* (M. Frey & D. Robinson, editors). Blackwell Science, Oxford, UK.

Meunier A., Inoue A. & Beaufort D. (1991) Chemiographic analysis of trioctahedral smectite-to-chlorite conversion series from the Ohyu Caldera, Japan. *Clays and Clay Minerals*, **39**, 409–415.

Milu V., Milesi J.P. & Leroy J.L. (2004) Rosia Poieni copper deposit, Apuseni Mountains, Romania: Advanced argillic overprint of a porphyry system. *Mineralium Deposita*, **39**, 173–188.

Moore D.M. & Reynolds R.C. Jr. (1997) *X-ray Diffraction and the Identification and Analysis of Clay Minerals*, 2nd edition. Oxford University Press, New york, 378 pp.

Morrison S.J. & Parry W.T. (1986) Dioctahedral corrensite from Permian red beds, Libson Valley, Utah. *Clays and Clay Minerals*, **34**, 613–624.

Morse J.W. & Casey W.H. (1988) Ostwald processes and mineral paragenesis in sediments. *American Journal of Science*, **288**, 537–560.

Murakami T., Sato T. & Inoue A. (1999) HRTEM evidence for the process and mechanism of saponite-to-chlorite conversion through corrensite. *American Mineralogist*, **84**, 1080–1087.

Norman D.K., Parry W.T. & Bowman J.R. (1991) Petrology and geochemistry of propylitic alteration at southwest Tintic, Utah. *Economic Geology*, **86**, 13–28.

Nutt C.J. (1989) Chloritization and associated alteration at the Jabiluka unconformity-type deposit, Northern Territory, Australia. *The Canadian Mineralogist*, **27**, 41–58.

Odin G.S. (1988) *Green marine clays; oolitic ironstone facies, verdine facies, glaucony facies and celadonite-bearing rock facies, a comparative study.* Developments in Sedimentology, **45**, Elsevier, Amsterdam, 445 pp.

Odin G.S. (1990). Clay mineral formation at the continent–ocean boundary: the verdine facies. *Clay Minerals*, **25**, 477–485.

Parthasarathy G., Choudary B.M., Sreedhar B., Kunwar A.C. & Srinivasan R. (2003) Ferrous saponite from the Deccan Trap, India, and its application in adsorption and reduction of hexavalent chromium. *American Mineralogist*, **88**, 1983–1988.

Patrier P., Papapanagiotou P., Beaufort D., Traineau H., Bril H. & Rojas J. (1996) Role of permeability versus temperature in the distribution of the fine (<0.2 µm) clay fraction in the Chipilapa geothermal system (El Salvador, Central America). *Journal of Volcanology and Geothermal Research*, **72**, 101–120.

Patrier P., Beaufort D. & Bruneton P. (2003) Dickite and $2M_1$ illite in deeply buried sandstones from the middle

Proterozoic Kombolgie Formation (Northern Territory, Australia). *Clays and Clay Minerals*, **51**, 102–116.

Percival J.B. & Kodama H. (1989) Sudoite from Cigar Lake, Saskatchewan. *The Canadian Mineralogist*, **27**, 633–641.

Peyraud J.B. & Worden R.H. (2007) The bioclay factory: digestion as a clay-generating process. Pp. 533–536 in: *Proceedings of the 12th Water-Rock Interaction conference* (T.D. Bullen & X. Wang. editors). Taylor and Francis, Kunming, China.

Pirajno F. (1992) *Hydrothermal Mineral Deposits. Principles and Fundamental Concepts for the Exploration Geologist.* Springer-Verlag, Berlin, 709 pp.

Porrenga D.H. (1967) Glauconite and chamosite as depth indicators in the marine environment. *Marine Geology*, **5**, 495–501.

Putnis A. (1992) *An Introduction to Mineral Sciences.* Cambridge, Cambridge University Press, 457 pp.

Putnis A. (2002) Mineral replacement reactions: From macroscopic observations to microscopic mechanisms. *Mineralogical Magazine*, **66**, 689–708.

Reynolds R.C. Jr. (1988) Mixed layer chlorite minerals. Pp. 601–630 in: *Hydrous Phyllosilicates (Exclusive of Micas)* (S.W. Bailey, editor). Reviews in Mineralogy, **19**, Mineralogical Society of America, Washington DC.

Reynolds R.C. Jr, Distefano M.P. & Lahann R.W. (1992) Randomly interstratified serpentine/chlorite: its detection and quantification by powder X-ray diffraction methods. *Clays and Clay Minerals*, **40**, 262–268.

Reeder J.W. (1985) Formation of geothermal resources at lithospheric subduction zones. *Energy Research*, **9**, 229–239.

Roberson H.E., Reynolds R.C. & Jenkins D.M. (1999) Hydrothermal synthesis of corrensite; a study of the transformation of saponite to corrensite. *Clays and Clay Minerals*, **47**, 212–218.

Rohrlich V., Price N.B. & Calvert S.E. (1969) Chamosite in recent sediments of Loch Etive, Scotland. *Journal of Sedimentary Petrology*, **39**, 624–631.

Ruiz Cruz M.D. & Sanz de Galdeano C. (2005). Compositional and structural variation of sudoite from the Betic Cordillera (Spain): A TEM/AEM study. *Clays and Clay Minerals*, **53**, 639–652.

Ryan P.C. & Hillier S. (2002) Berthierine/chamosite, corrensite, and discrete chlorite from evolved verdine and evaporite-associated facies in the Jurassic Sundance Formation, Wyoming. *American Mineralogist*, **87**, 1607–1615.

Ryan P.C. & Reynolds R.C. Jr. (1996) The origin and diagenesis of grain-coating serpentine-chlorite in Tuscaloosa Formation sandstone, U.S. *Gulf Coast. American Mineralogist*, **81**, 213–225.

Ryan P.C. & Reynolds R.C. Jr. (1997) The chemical composition of serpentine/chlorite in the Tuscaloosa formation, United States Gulf coast: EDX vs. XRD determinations, implications for mineralogic reactions and the origin of anatase. *Clays and Clay Minerals*, **45**, 339–352.

Schiffman P. & Fridleifsson G.O. (1991) The smectite-chlorite transition in drill hole NJ-15, Nesjavellir geothermal field, Iceland: XRD, BSE and electron microprobe investigations. *Journal of Metamorphic Geology*, **9**, 679–696.

Schiffman P. & Staudigel H. (1995) The smectite to chlorite transition in a fossil seamount hydrothermal system: the basement complex of La Palma, Canary Islands. *Journal of Metamorphic Geology*, **13**, 487–498.

Schultz L.G. (1963) Clay minerals in Triassic rocks of the Colorado Plateau. *U.S. Geological Survey Professional Paper* **1147-C**, p. C1–C71.

Shau Y.H. & Peacor D.R. (1992) Phyllosilicates in hydrothermally altered basalts from DSDP Hole 504B, Leg 83 – a TEM and AEM study. *Contributions to Mineralogy and Petrology*, **112**, 119–133.

Shau Y.H., Peacor D.R. & Essene E.J. (1990) Corrensite and mixed-layer chlorite/corrensite in metabasalt from northern Taiwan: TEM/AEM, EMPA, XRD, and optical studies. *Contributions to Mineralogy and Petrology*, **105**, 123–142.

Shikazono N. & Kawahata H. (1987) Compositional differences in chlorite from hydrothermally altered rocks and hydrothermal ore deposits. *The Canadian Mineralogist*, **25**, 465–474.

Schmidt D. & Livi K.J.T. (1999) HRTEM and SAED investigations of polytypism, stacking disorder, crystal growth, and vacancies in chlorite from subgreenschist facies outcrops. *American Mineralogist*, **84**, 160–170.

Schmidt S.T. & Robinson D. (1997) Metamorphic grade and porosity/permeability controls on mafic phyllosilicate distributions in a regional zeolite to greenschist facies transition of the North Shore Volcanic Group, Minnesota. *Bulletin of the Geological Society of America*, **109**, 683–697.

Shirozu H. (1978) Chlorite minerals. Pp. 243–264 in: *Clays and Clay Minerals of Japan* (T. Sudo & S. Shimoda, editors). Developments in Sedimentology, **26**. Elsevier, Amsterdam and London.

Simmons S.F. & Browne P.R.L. (2000) Hydrothermal minerals and precious metals in the Broadlands-Ohaaki geothermal system: Implications for understanding low-sulfidation epithermal environments. *Economic Geology*, **95**, 971–999.

Slack J.F., Jiang W.T., Peacor D.R. & Okita P.M. (1992) Hydrothermal and metamorphic berthierine from the Kidd Creek volcanogenic massive sulfide deposit, Timmins, Ontario. *The Canadian Mineralogist*, **30**, 1127–1149.

Smith F.W. & Hardy R.G. (1981) Clay minerals in the veins of the North Pennine orefield, UK. *Clay Minerals*, **16**, 309–312.

Sudo T. & Sato M. (1966) Dioctahedral chlorite. *Proceedings of the International. Clay Conference* (L. Heller & A. Weiss, editors), **1**, 33–39, Jerusalem.

Sudo T. & Shimoda S. (editors) (1978) *Clays and Clay Minerals of Japan.* Developments in Sedimentology, **26**. Elsevier, Amsterdam and London.

Sugimori H., Iwatsuki T. & Murakami T. (2008) Chlorite and biotite weathering, Fe^{2+}-rich corrensite formation, and Fe behavior under low PO_2 conditions and their implication for Precambrian weathering. *American Mineralogist*, **93**, 1080–1089.

Teklemariam M., Battaglia S., Gianelli G. & Ruggieri G. (1996) Hydrothermal alteration in the Aluto-Langano geothermal field, Ethiopia. *Geothermics*, **25**, 679–702.

Theye T., Seidel E. & Vidal O. (1992) Carpholite, sudoite and chloritoid in low-grade high-pressure metapelites from Crete and the Peloponnese, Greece. *European Journal of Mineralogy*, **4**, 487–507.

Tompkins R.E. (1981) Scanning electron microscopy of a regular chlorite/smectite (corrensite) from a hydrocarbon reservoir sandstone. *Clays and Clay Minerals*, **29**, 233–235.

Van Houten F.B. & Purucker M.E. (1984) Glauconite peloids and chamositic ooids – favorable factors, constraints and problems. *Earth Science Review*, **20**, 211–243.

Veblen D.R. (1992) Electron microscopy applied to nonstoichiometry polysomatism and replacement reactions in minerals. Pp. 181–229 in: *Mineral Reactions at the Atomic Scale: Transmission Electron Microscopy* (P. Buseck, editor). Reviews in Mineralogy, **27**, Mineralogical Society of America, Washington, D.C.

Velde B. (1985) *Clay Minerals: A Physico-chemical Explanation of their Occurrence*. Elsevier Amsterdam, 427 pp.

Velde B. & Lanson B. (1993) Comparison of I/S transformation and maturity of organic matter at elevated temperatures. *Clays and Clay Minerals*, **41**, 178–183.

Vidal O. & Dubacq B. (2009) Thermodynamic modelling of clay dehydration, stability and compositional evolution with temperature, pressure and H_2O activity. *Geochimica et Cosmochimica Acta*, **73**, 6544–6564.

Vidal O., Goffe B. & Theye T. (1992) Experimental study of the stability of sudoite and magnesiocarpholite and calculation of a new petrogenetic grid for the system $FeO\text{-}MgO\text{-}Al_2O_3\text{-}SiO_2\text{-}H_2O$. *Journal of Metamorphic Petrology*, **10**, 603–614.

Vidal O., Parra T. & Trotet F. (2001) A thermodynamic model for Fe-Mg aluminous chlorite using data from phase equilibrium experiments and natural pelitic assemblages in the 100°C to 600°C, 1 to 25 kb range. *American Journal of Science*, **301**, 557–592.

Vidal O., Parra T. & Vieillard P. (2005) Thermodynamic properties of the Tschermak solid solution in Fe-chlorite: Application to natural examples and possible role of oxidation. *American Mineralogist*, **90**, 347–358.

Vidal O., Baldeyrou A., Beaufort D., Fritz B., Geoffroy N. & Lanson B. (2012) Experimental study of the stability and phase relations of clays at high temperature in a thermal gradient. *Clays and Clay Minerals*, **60**, 200–225.

Walker J.R. (1993) Chlorite polytype geothermometry. *Clays and Clay Minerals*, **41**, 260–267.

Walker J.R. & Thompson G.R. (1990) Structural variations in chlorite and illite in a diagenetic sequence from the Imperial Valley, California. *Clays and Clay Minerals* **38**, 315–321.

Walshe J.L. (1986) A six-component chlorite solid solution model and the conditions of chlorite formation in hydrothermal and geothermal systems. *Economic Geology*, **81**, 681–703.

Whittle C.K. (1986) Comparisons of sedimentary chlorite compositions by X-ray diffraction and analytical TEM. *Clay Minerals*, **21**, 937–947.

Wiewióra A. & Weiss Z. (1990) Crystallochemical classifications of phyllosilicates based on the unified system of projection of chemical composition: II. The chlorite group. *Clay Minerals*, **25**, 83–92.

Wilson M.J. (1971) Clay mineralogy of the Old Red Sandstone (Devonian) of Scotland. *Journal of Sedimentary Petrology*, **41**, 995–1007.

Worden R.H. & Morad S. (2003) Clay minerals in sandstones: control on formation, distribution and evolution. *International Association of Sedimentologists, Special Publication*, **34**, 3–41.

Xu H. & Veblen D.R. (1996) Interstratification and other reaction microstructures in the chlorite–berthierine series. *Contributions to Mineralogy and Petrology*, **124**, 291–301.

Yau Y.C., Peacor D.R., Beane R.E., Essene E.J. & McDowell S.D. (1988) Microstructures, formation mechanisms, and depth zoning of phyllosilicates in geothermally altered shales, Salton Sea, California. *Clays and Clay Minerals*, **36**, 1–10.